Journal of Sound and Vibration (2000) **238**(5), 809–851
doi:10.1006/jsvi.2000.3137, available online at http://www.idealibrary.com on IDEAL®

DYNAMIC STABILITY OF COLUMNS SUBJECTED TO FOLLOWER LOADS: A SURVEY

M. A. LANGTHJEM

Institute of Mechanical Engineering, Aalborg University, Pontoppidanstræde 101, *DK*-9220 *Aalborg East, Denmark. E-mail: ml@ime.auc.dk*

AND

Y. SUGIYAMA

Department of Aerospace Engineering, Osaka Prefecture University, 1-1 *Gakuen-cho, Sakai-shi*, 599-8531 *Osaka, Japan. E-mail: sugiyama@aero.osakafu-u.ac.jp*

(*Received* 19 *May* 2000)

This paper offers a survey of simple, flexible structural elements subjected to non-conservative follower loads, such as those caused by the thrust of rocket- and jet engines, and by dry friction in automotive disk- and drum-brake systems. Emphasis is on the "canonical problems", Beck's, Reut's, Leipholz's, and Hauger's columns. Beck's and Reut's columns have been realized experimentally, and very good agreement between theory and experiments has been found. Leipholz's column is basically realized in an automobile brake system, where noise due to dynamic or parametric instability (brake squeal) is a well-known environmental problem. It is attempted to give a broad overview, with emphasis on experimental works and the associated theoretical problems. Structural optimization is also included in the review, as many studies in that area have served an important purpose in the development of optimization techniques for practical, large-scale optimization problems with non-conservative forces, such as in aeroelasticity.

1. INTRODUCTION

1.1. MODELS CONSIDERED IN THIS PAPER

This paper surveys simple structural elements under non-conservative "follower" loads, such as those caused by rocket- and jet engines, and by dry friction in automotive disk- and drum-brake systems. Emphasis is on the so-called Beck's, Reut's, Leipholz's, and Hauger's columns, and their generalizations.

Beck's column is a cantilever subjected to a tangential follower load at the free end. Reut's column is compressed by a force with a fixed line of action (the *undeformed* beam axis), acting on a completely rigid cross-beam, attached at the free end of the cantilever. Leipholz's column has a uniformly distributed follower loading along its span, while Hauger's column has a linearly (towards the clamped end) increasing distributed follower load. Follower force loaded free–free beams and plates are also included in the survey. They are typically used as simple models of missiles, rockets and space structures, such as solar panels.

One of the most easily realized follower force systems is a cantilevered pipe conveying fluid. A very comprehensive review of fluid-conveying pipes has been given by Païdoussis

0022-460X/00/500809 + 43 $35.00/0

and Li [1] and the subject has been treated in more detail by Païdoussis [2]. Fluid-conveying pipes will therefore not be considered here.

Studies within the subject of the present survey have from time to time been criticized as being purely theoretical and having no relevance to practical engineering problems [3, 4]. Some recent papers have attempted to justify and explain the basic ideas [5, 6], and it is also one of the main purposes of this paper.

Admittedly, many published papers on problems with follower forces *do* have a strong theoretical and mathematical bias. Often, the underlying physical problem (if any) has been oversimplified [7]. But still, many of these studies are very interesting from a *general theory of dynamic stability* point of view, and studies of simple follower force systems help to obtain a deeper understanding of much more complex practical/industrial stability problems.

The mechanical systems reviewed here may be said to be the simplest flutter-prone continuous structures. Beck's column [8], and the related systems, have received so much research attention because of their interesting dynamic behavior. The governing equations for flutter of aircraft wings, cantilevered fluid-conveying pipes, and cantilevered columns subject to a rocket thrust, have the same mathematical form. Of course, the simple Beck's column cannot completely "capture" the very complex problem of aircraft flutter. But if the focus is on the passage through the stability boundary, and on the energy balance between dissipative and circulatory forces, then much can be learned from studies of simple systems. Bishop and Fawzy [9] studied the dynamics of a cantilevered fluid-conveying tube and wrote:

"The studies reported in this paper were conceived as a possible means of investigating a technical problem of extreme importance, namely the flutter of aircraft. It is not suggested, of course, that a vertical tube conveying a liquid bears much resemblance to an aircraft in flight, but such similarities as there are, are perhaps worthy of some thought. To study the phenomena that are normally associated with flutter and flight flutter testing, and to which simple flutter calculations apply, it would evidently be helpful to consider a much simpler system than an aircraft."

This point of view also applies to the mechanical systems reviewed in the present paper. But flutter of Beck's column may be more related to flutter of aircraft than flutter of a cantilevered fluid-conveying tube, since Beck's column and aircraft are not subject to such heavy fluid damping as the fluid-conveying tube is.

Several reviews of problems involving follower forces have been published. Herrmann wrote general reviews in 1967 [10] and in 1971 [3]. Sugiyama and Sekiya [11] reviewed the experimental works with follower forces in 1971. Another general review was given by Sundararajan [12] in 1975. Weisshaar and Plaut [13] reviewed optimum design of structures subjected to follower loads in 1981. Seyranian [14] gave a comprehensive review of studies into the effects of damping in 1990, addressing especially the possible destabilizing effect. Recently, Bolotin [6] gave a retrospective on the important developments in dynamic stability theory.

A very interesting review on "real" aircraft flutter was published by Garrick and Reed [15]. That paper describes practical problems with flutter, from the Wright Brothers to supersonic aircraft, and the means of curing the problems, with the aid of computations and model testing.

Several books dealing with follower force loaded structures have been published, and some include comprehensive reviews up to the year of publication. Among the most popular are those by Bolotin [16], Panovko and Gubanova [17], Ziegler [18], Huseyin [19], Leipholz [20], El Naschie [21], and Bazant and Cedolin [22]. Gajewski and Zyczkowski [23] wrote a book dealing with optimization of structures subjected to stability constraints, which also includes a comprehensive review and publication list on the subject.

1.2. STRUCTURE OF THE PAPER

This is not a concise catalogue of work within the area. However, an attempt is made to give a broad overview. Emphasis is on recent developments, but early, pioneering papers are also included. Experimental works are particularly emphasized. Another area which is emphasized is structural optimization.

Section 2 is concerned with linear stability analysis. Sections 2.1–2.4 review the equations for linear dynamic stability of generalized Beck's, Reut's, Leipholz's, and Hauger's columns. Stability analysis is discussed in sections 2.5–2.7. Sections 2.8–2.11 discuss the effects of damping, boundary conditions and load distribution. Section 2.12 gives a discussion of the energetics at the stability limit.

Section 3 reviews experimental works. Section 3.1 is concerned with Reut's column, while Beck's column is the subject of section 3.2.

Section 4 is concerned with optimum design of columns subjected to follower loads. Section 5 deals with parametric instability, section 6 with non-linear dynamics, and section 7 with plates under follower loading. Section 8 discusses finite load increase (contrary to a quasistatic increase). Finally, some conclusions are made in section 9.

2. BASIC LINEAR DYNAMICS AND STABILITY

2.1. BECK'S COLUMN IN GENERALIZED FORM

A generalized form of Beck's column, with an end-mass of finite size, was introduced by Wood *et al.* [24] (see Figure 1). Here we consider a (possibly) non-uniform, *standing* column of viscoelastic material, vibrating in a viscous medium. The equation of motion is

$$\frac{\partial}{\partial x^2}\left\{EI\frac{\partial^2 y}{\partial x^2}+E^*I\frac{\partial}{\partial t}\left(\frac{\partial^2 y}{\partial x^2}\right)\right\}-gm\frac{\partial y}{\partial x}+g\frac{\partial^2 y}{\partial x^2}\int_x^L m(\xi)\,\mathrm{d}\xi$$

$$+(p+Mg)\frac{\partial^2 y}{\partial x^2}+C\frac{\partial y}{\partial t}+m\frac{\partial^2 y}{\partial t^2}=0. \tag{1}$$

Here $y=y(x,t)$ is the transverse displacement at position x, t is the time, $m=m(x)$ is the mass per unit length, p is the mean thrust, $EI=EI(x)$ is the flexural rigidity of the column (E is the modulus of elasticity and I is the area moment of inertia), E^* is the coefficient of dynamic visco-elastic resistance [25, 26], M is the endmass, J is the corresponding rotatory inertia, g is the gravity acceleration, and C is the coefficient of external viscous damping. This coefficient is proportional to the width (or diameter) of the column [27]. If the column is clamped at $x=0$ and free at $x=L$, the boundary conditions are

$$y=0 \quad \text{and} \quad \frac{\partial y}{\partial x}=0 \quad \text{at } x=0,$$

$$EI\frac{\partial^2 y}{\partial x^2}+E^*I\frac{\partial}{\partial t}\left(\frac{\partial^2 y}{\partial x^2}\right)-Mg\frac{\partial y}{\partial x}a+M\frac{\partial^2}{\partial t^2}\left(y+a\frac{\partial y}{\partial x}\right)a+J\frac{\partial^2}{\partial t^2}\left(\frac{\partial y}{\partial x}\right)=0 \quad \text{and}$$

$$\frac{\partial}{\partial x}\left\{EI\frac{\partial^2 y}{\partial x^2}+E^*I\frac{\partial}{\partial t}\left(\frac{\partial^2 y}{\partial x^2}\right)\right\}+Mg\frac{\partial y}{\partial x}-M\frac{\partial^2}{\partial t^2}\left(y+a\frac{\partial y}{\partial x}\right)=0 \quad \text{at } x=L, \tag{2}$$

where a is the distace from the column end to the center of gravity of the end-mass.

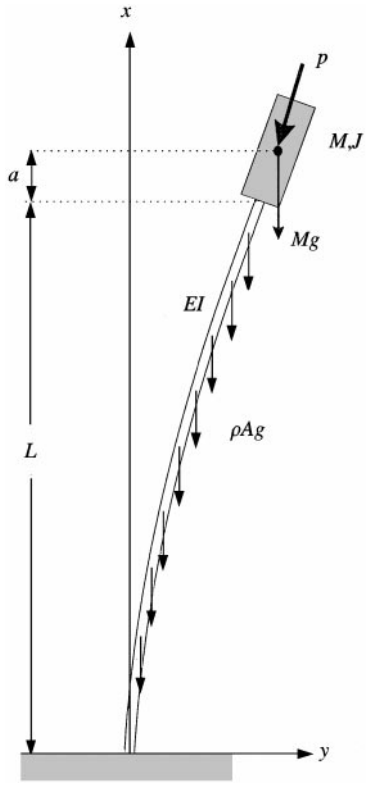

Figure 1. Generalized, standing Beck's column. The non-conservative follower force, of magnitude p, may be generated by the thrust of a solid-propellant rocket motor [36, 56, 57], or by a water jet issued from a nozzle box [24] (see section 3, and Figures 10, 12, 13 and 15). The rocket motor (or nozzle box) has mass M and rotatory inertia J. The column is of length L, and it has stiffness EI, cross-section area A and density ρ. The distance from the column end to the center of gravity of the rocket motor (or nozzle box) is denoted by a.

2.2. LEIPHOLZ'S AND HAUGER'S COLUMNS

The cantilevered column with a uniformly distributed follower force p' (force per unit length) is usually referred to as Leipholz's column. Hauger's column has a self-weight-like force distribution, which varies linearly from 0 at the top to p' at the clamping. The equations of motion are obtained by replacing $p\,\partial^2 y/\partial x^2$ with $p'Q(x)\,\partial^2 y/\partial x^2$ in equation (1) where $Q(x)$ is a force distribution function, which is

$$Q = L\int_{x/L}^{1} 1\,\mathrm{d}\bar{\xi} = L - x \tag{3}$$

for Leipholz's column [28] and

$$Q = L\int_{x/L}^{1} (1-\bar{\xi})\,\mathrm{d}\bar{\xi} = \frac{L}{2}(1-x/L)^2 \tag{4}$$

for Hauger's column [29].

The uniformly distributed follower forces have their origin in several engineering problems. One example is the friction forces on the wall of a tube caused by a creeping (very slow) flow of a highly viscous fluid [30]. The Reynolds number

$$\mathrm{Re} = \frac{\text{inertia forces}}{\text{viscous forces}} \tag{5}$$

is thus very small.

Another example is the friction forces acting on slender cylinders in axial flow, including flying rockets and missiles [31, 32].

A third example is automotive disc- and drum-brake systems. Kang and Tan [33] showed that the equation of motion governing the vibrations of a disk brake pad under the action of a rotating brake disk is *identical* with the equation of motion for Leipholz's column. The onset of brake "squeal" is thus caused by a flutter instability, or by a parametric instability (see section 5).

Engineering problems which similarly reduce to Hauger's column have yet to be reported. But with a view to reference [33], it might be related to a non-perfect automotive brake system, where the tread of the brake pad on the disc is not uniform (due to oil, wear, etc.).

2.3. BOUNDARY VALUE PROBLEM

By inserting a displacement of the form

$$y(x, t) = \tilde{y}(x)\exp(\lambda t), \quad \lambda = \alpha + \mathrm{i}\omega \quad (\mathrm{i} = \sqrt{-1}) \tag{6}$$

and introducing the non-dimensional variables

$$\bar{x} = \frac{x}{L}, \quad \bar{y} = \frac{\tilde{y}}{L}, \quad \bar{\xi} = \frac{\xi}{L}, \quad P = p + Mg, \quad \bar{p} = \frac{PL^2}{EI_0},$$

$$\mu = \frac{M}{m_0 L}, \quad \gamma = g\frac{m_0 L^3}{EI_0}, \quad \bar{m} = \frac{m}{m_0}, \quad \bar{s} = \frac{I}{I_0}, \quad \bar{a} = \frac{a}{L}, \quad \eta = \frac{p}{P},$$

$$\bar{J} = \frac{J}{m_0 L^3}, \quad \bar{t} = \frac{t}{L^2}\sqrt{\frac{EI_0}{m_0}}, \quad \bar{\lambda} = \frac{t}{\bar{t}}\lambda, \quad \beta = \frac{CL^2}{\sqrt{EI_0 m_0}}, \quad \sigma = \frac{E^*}{EL^2}\sqrt{\frac{EI_0}{m_0}}, \tag{7}$$

equations (1) and (2) are converted into the following non-dimensional boundary value problem:

$$B[y] = \{(1 + \lambda\sigma)sy''\}'' + \left(\gamma\int_x^1 m(\xi)\,\mathrm{d}\xi + p\right)y'' - \gamma m y' + \lambda(\beta + \lambda m)y = 0,$$

$$y = 0 \quad \text{and} \quad y' = 0 \quad \text{at } x = 0,$$

$$(1 + \lambda\sigma)sy'' + \{\lambda^2(J + a^2\mu) - ap(1 - \eta)\}y' + \lambda^2 a\mu y = 0 \quad \text{and}$$

$$\{(1 + \lambda\sigma)sy''\}' + \{p(1 - \eta) - \lambda^2 a\mu\}y' - \lambda^2\mu y = 0 \quad \text{at } x = 1, \tag{8}$$

where in the differential operator $B[\ ]$ has been defined. All "overbars" have again been dropped, for the sake of simple notation.

It is noted that $\eta = 0$ corresponds to a pure conservative end-loading and $\eta = 1$ to a pure tangential non-conservative end-loading. A value $0 < \eta < 1$ is often called a *partial*, or *sub-tangential* follower load, and the parameter η is often called the non-conservativeness parameter.

A *partial*, *distributed* follower load may also be obtained, for example, due to the combined action of viscous fluid forces in a pipe and self-weight (i.e., gravity forces). This has been studied by Sugiyama and Kawagoe [34], and by Sugiyama and Mladenov [30] (see also section 2.9).

2.4. REUT'S COLUMN IN GENERALIZED FORM

This column is sketched in Figure 2 with a finite-size end-mass included. It has exactly the same stability limit as the generalized Beck's column, since the boundary value problem describing small vibrations of this column is adjoint to equation (8). It is obtained from the identity

$$\int_0^1 [vB[y] - yR[v]]\,\mathrm{d}x = 0. \tag{9}$$

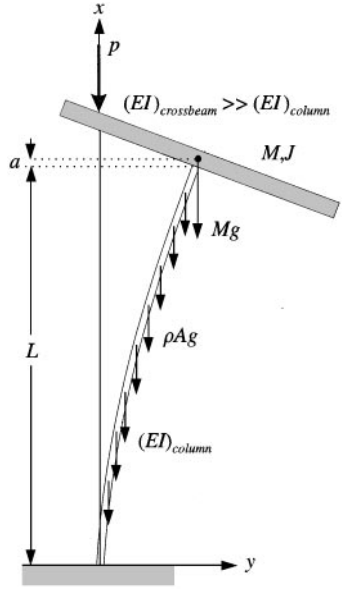

Figure 2. Generalized, standing Reut's column. The non-conservative follower force p may be generated by an air jet, impinging onto an almost rigid crossbeam [102–104] (see Section 3, and Figure 9). In order to obtain the situation shown, the crossbeam must be covered with a "non-reflecting", coarse material. The symbols are similar to those used and defined in Figure 1.

This equation is satisfied if

$$R[v] = \{(1 + \lambda\sigma)sv''\}'' + \left(\gamma\int_x^{\prime} m(\xi)\mathrm{d}\xi + p\right)v'' - \gamma m v'\lambda(\beta + \lambda m)v = 0,$$

$$v = 0 \quad \text{and} \quad v' = 0 \quad \text{at } x = 0,$$

$$(1 + \lambda\sigma)sv'' + \{\lambda^2(J + a^2\mu) - ap(1 - \eta)\}v' + (p\eta + \lambda^2 a\mu)v = 0 \quad \text{and}$$

$$\{(1 + \lambda\sigma)sv''\}' + pv' - \lambda^2\mu(av' + v) = 0 \quad \text{at } x = 1. \tag{10}$$

2.5. SEMI-ANALYTICAL SOLUTION OF THE BOUNDARY VALUE PROBLEM

It is possible to obtain a semi-analytical solution to the boundary value problem for the generalized Beck's/Reut's column with uniform mass and stiffness distributions, $m(x) \equiv 1$ and $s(x) \equiv 1$ respectively. Considering Beck's column, a solution of the form

$$y(x) = k\exp(\zeta x) \tag{11}$$

satisfies equation (8). Inserting this expression into the differential equation gives a fourth order polynomial in ζ. After having determined the four roots ζ_1, ζ_2, ζ_3 and ζ_4, the general solution to the fourth order ordinary differential equation (8) can be written as

$$y(x) = \sum_{n=1}^{4} k_n \exp(\zeta_n x). \tag{12}$$

Inserting expression (12) into the boundary conditions in equations (8) gives a matrix equation system of the form

$$\mathbf{Bk} = \mathbf{0}, \tag{13}$$

where $\mathbf{B}$ is a 4×4 matrix, where the coefficients are functions of the non-dimensional parameters (7) and $\mathbf{k}$ is a column vector. A non-trivial solution requires that

$$\det \mathbf{B} = 0. \tag{14}$$

This gives a transcendent equation from which the eigenvalues λ can be obtained by using an iterative method [8, 35, 36]. Pedersen [35] obtained an elegant formulation of equation (14) by expressing the solution (12) in terms of simple and hyperbolic cosine and sine functions, rather than in exponentials, and by introducing some auxiliary, complex functions. Morgan and Sinha [37] used this formulation to obtain a semi-analytical solution for Beck's column on a continuous viscoelastic foundation (see also section 2.8).

By using the method of *transfer matrices*, a semi-analytical solution can in fact also be found if the cross-sections have just piecewise constant thickness [38]. Distributed elastic supports may also be included.

2.6. DISCRETIZATION

If the column has non-uniform sections, or if the load is distributed, a discretization method must be applied. (However, semianalytical methods have been proposed; see, e.g., reference [39].)

Prasad and Herrmann [40, 41] and Anderson [42] have studied the usefulness of the adjoint system (10) when determining eigensolutions to (8), and *vice versa*. By using

equations (8) and (10), one can obtain the functional

$$\mathscr{L}(y,v) = \lambda^2\left[\int_0^1 myv\,\mathrm{d}x + \mu\{yv + a(yv' + y'v) + (J/\mu + a^2)y'v'\}_{x=1}\right]$$
$$+ \lambda\left[\sigma\int_0^1 sy''v''\,\mathrm{d}x + \int_0^1 \beta yv\,\mathrm{d}x\right] + \int_0^1\left[sy''v'' - \gamma\int_x^1 m(\xi)\,\mathrm{d}\xi y'v'\right]\mathrm{d}x$$
$$+ p\left[\eta\{y'v\}_{x=1} - \int_0^1 y'v'\,\mathrm{d}x - a(1-\eta)\{y'v'\}_{x=1}\right], \tag{15}$$

which is stationary with respect to variations δy, δv just satisfying the kinematic boundary conditions $y(0) = 0$ and $y'(0) = 0$ (and $v(0) = 0, v'(0) = 0$). This functional is a sound basis for the discretization. With any discretization method, the discretized equation of motion takes the form

$$\mathbf{L}\mathbf{y} = [\lambda^2\mathbf{M} + \lambda\mathbf{C} + \mathbf{K} + p\mathbf{Q}]\mathbf{y} = \mathbf{0}, \tag{16}$$

where $\mathbf{M}$ is the mass matrix, $\mathbf{C}$ is the damping matrix, $\mathbf{K}$ is the stiffness matrix, and $\mathbf{Q}$ is the load matrix. $\mathbf{L}$ is termed the system matrix. $\mathbf{M}$ is obtained from the first square bracket in equation (15), $\mathbf{C}$ is obtained from the second, $\mathbf{K}$ is obtained from the third, and lastly, $\mathbf{Q}$ is obtained from the fourth square bracket in equation (15). Thus, the matrices $\mathbf{M}$, $\mathbf{C}$ and $\mathbf{K}$ are symmetric, while $\mathbf{Q}$ is non-symmetric.

The discretized adjoint system has the form

$$\mathbf{L}^{\mathrm{T}}\mathbf{v} = [\lambda^2\mathbf{M} + \lambda\mathbf{C} + \mathbf{K} + p\mathbf{Q}]^{\mathrm{T}}\mathbf{v} = \mathbf{0}. \tag{17}$$

Properties of, and techniques for, non-symmetric matrices, with emphasis on non-conservative vibratory systems, have been studied by Lancaster [43], and by Fawzy and Bishop [44]. One of the most important results in reference [44] is the biorthogonality condition for the eigensolutions $(\lambda_{\mathbf{y}}, \mathbf{y})$ and $(\lambda_{\mathbf{v}}, \mathbf{v})$. They are orthogonal in the following way:

$$\mathbf{v}^{\mathrm{T}}[(\lambda_{\mathbf{y}} + \lambda_{\mathbf{v}})\mathbf{M} + \mathbf{C}]\mathbf{y} = 0. \tag{18}$$

It may be noted that the biorthogonality condition for the continuous eigensolutions $(\lambda_y, y(x))$ and $(\lambda_v, v(x))$ is given by

$$\int_0^1 [\sigma sy''v'' + \{\beta + (\lambda_y + \lambda_v)m\}yv]\,\mathrm{d}x + (\lambda_y + \lambda_v)\mu[yv + a(yv' + y'v) + (J/\mu + a^2)y'v']_{x=1} = 0. \tag{19}$$

In order to determine the eigenvalues, equation (16) is normally rewritten as

$$\left(\begin{bmatrix} \mathbf{0} & \mathbf{I} \\ -p\mathbf{Q} - \mathbf{K} & -\mathbf{C} \end{bmatrix} - \lambda\begin{bmatrix} \mathbf{I} & \mathbf{0} \\ \mathbf{0} & \mathbf{M} \end{bmatrix}\right)\begin{Bmatrix} \mathbf{y} \\ \lambda\mathbf{y} \end{Bmatrix} = 0. \tag{20}$$

This equation can then be transformed into a standard linear eigenvalue problem,

$$\mathbf{A}\mathbf{q} = \lambda\mathbf{q}, \tag{21}$$

where

$$\mathbf{A} = \begin{bmatrix} \mathbf{0} & \mathbf{I} \\ -\mathbf{M}^{-1}(p\mathbf{Q}+\mathbf{K}) & -\mathbf{M}^{-1}\mathbf{C} \end{bmatrix} \quad \text{and} \quad \mathbf{q} = \begin{Bmatrix} \mathbf{y} \\ \lambda\mathbf{y} \end{Bmatrix}. \tag{22}$$

Prasad and Herrmann [41] discussed the Galerkin method and the method of least squares. Leipholz [20] gave a very thorough discussion of the Galerkin method, including the question of convergence. Application of *the finite element method* to eigenvalue analysis for Beck's column was published almost simultaneously by Mote Jr [45] and Barsoum [46].

2.7. STABILITY CRITERIA

One of the most used definitions of stability is Lyapunov's definition; see, e.g., references [16, 47]. For small periodic vibrations (with frequency ω) about equilibrium of beams, a solution has form (6). Application of Lyapunov's stability definition gives that the vibrations are stable if all $\alpha \leqslant 0$, asymptotically stable if all $\alpha < 0$, and unstable if at least one $\alpha > 0$. The instability is termed divergence if $\omega = 0$ for the unstable eigenvalue(s), and flutter if $\omega \neq 0$.

Figure 3 shows the stability boundaries for the generalized Beck's column, as a function of the non-conservativeness parameter η, for different damping parameters. Divergence occurs for $\eta < 0{\cdot}5$ and flutter for $\eta > 0{\cdot}5$. For the model without damping, there is an isolated divergence load at $\eta = 0{\cdot}5$. Increasing the load beyond this value results in restabilization and then flutter. If small internal damping is included, divergence and flutter coincide at $\eta = 0{\cdot}5$. It is worth noticing that the stability map for the cantilever with a partial, distributed follower force is very similar [30, 34]. Also here, the divergence-flutter transition takes place at $\eta = 0{\cdot}5$.

Eigenvalue analysis of large, non-symmetric matrices can be very time consuming. Much work has been done on methods which give just a few eigenvalues with largest real parts α,

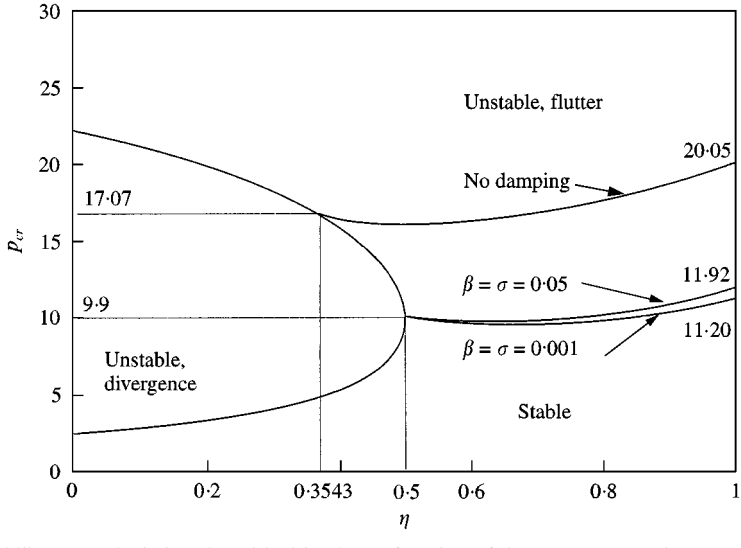

Figure 3. Stability map, depicting the critical load as a function of the non-conservativeness parameter η, for a cantilevered column loaded by a partial follower force, with various values of internal damping σ and external damping β.

sometimes called the *leading eigenvalues* [48–51]. But still, a method which is both robust and simple has not yet appeared. Ringertz [52] used a matrix formulation of Lyapunov's stability criterion, which eliminates the need for direct eigenvalue analysis. The criterion says that if all eigenvalues λ in the matrix $\mathbf{A}$ (equation (22)) have negative real parts, then there exists a symmetric, positive definite matrix $\mathbf{P}$ such that the matrix

$$[\mathbf{A}^{\mathrm{T}}\mathbf{P} + \mathbf{P}\mathbf{A}] \tag{23}$$

is negative definite. In reference [52] the condition for dynamic stability is then posed as follows. Let $\mathbf{R}$ be any positive-definite matrix (for example the unit matrix $\mathbf{I}$). All eigenvalues of $\mathbf{A}$ then have negative real parts, and the vibrations are stable, if the matrix $\mathbf{P}$ obtained from the Riccati equation

$$\mathbf{A}^{\mathrm{T}}\mathbf{P} + \mathbf{P}\mathbf{A} + \mathbf{R} = \mathbf{0} \tag{24}$$

is positive definite.†

Lyapunov's stability definition considers stability in an infinite interval of time. For practical applications, this may be too restrictive for systems with little damping, when the load is applied only in a short interval of time. This is related to the famous problem of the destabilizing effect of damping, which is treated in greater detail in the next section. Here it is sufficient to note that when both internal and external damping are small, the amplitude growth rate $\exp(\alpha t)$ is very small in the load range $p_{cr,\,damped} < p < p_{cr,\,undamped}$, where $p_{cr,damped}$ and $p_{cr,undamped}$ are the critical load values for the damped and the undamped columns, respectively. So although the system mathematically may be unstable (in the sense of Lyapunov) it may be considered as being stable for practical purposes. Herrmann and Jong [54] proposed a relaxed stability criterion based on a measure of the rate of amplitude growth during a period of oscillation. They defined the *logarithmic increment* as

$$\delta = \log \frac{A_n}{A_{n+1}}, \tag{25}$$

where A_n is the amplitude of the oscillation at time t, and A_{n+1} is the amplitude at time $t + T$, where T is the period. Using the exponential time dependence in equation (6) simply gives

$$\delta = -\alpha T = -2\pi \frac{\alpha}{\omega}. \tag{26}$$

Stable oscillations (in the sense of Lyapunov) exist if $\delta \geqslant 0$, and asymptotically stable oscillations if $\delta > 0$. In practical applications, δ may obtain a negative value within the duration of the loading without appreciable loss of stability.

A more comprehensive, practical stability criterion was suggested by Herrmann [55]. Here a *transition force* p_{T} is defined as the load where α would be "relatively small" for $p < p_T$ and "relatively large" for $p > p_T$. Herrmann suggests that the point where the $p(\alpha)$ curve has maximum curvature would be the natural definition of p_T.

These ideas have not been pursued further since their introduction, due to lack of experimental work. But they appear to be extremely useful for experimental systems like those of Sugiyama *et al.* [36, 56, 57] (see section 3), and ought to be followed up.

† A simple way of checking a symmetric matrix for positive definiteness is to perform a Cholesky decomposition (or attempt to — it is only possible when positive definite) [53].

Sugiyama *et al.* [36] suggested a slightly different criterion: the system is considered as being stable if small disturbances are amplified less than n times during the time interval t_l wherein the load acts. If α_{max} is the largest α value, the system is then considered as being stable if

$$\exp(\alpha_{max} t_l) < n. \tag{27}$$

The critical load p_{cr} is then defined as the load at which

$$\alpha_{max} = \frac{\ln(n)}{t_l}. \tag{28}$$

In conclusion to this section, the different relaxed stability criteria ought to be carefully compared and, if possible, unified.

2.8. THE EFFECT OF DAMPING

The destabilizing effect of small damping in structures subject to non-conservative loading is perhaps one of the most interesting problems in applied mechanics, and it has been studied very thoroughly since its discovery by Ziegler in 1952 [58]. Ziegler considered a two-degrees-of-freedom model (Ziegler's pendulum). Herrmann and Jong [54] showed that small Sezawa internal damping [25] in a continuous cantilever (Beck's column) may act destabilizing. Bolotin and Zhinzher [59] performed a very thorough parameter study of the continuous cantilever subjected to the combined action of a follower end load, and a dead (conservative) end load. Bolotin [60] gave a critical review of that work and discussed other mechanical systems where damping may act destabilizing. Herrmann [3] wrote a comprehensive review covering the works up till 1970.

Bolotin and Zhinzher [59] suggested a new terminology in dynamic stability, which is illustrated by Figure 4, adapted from reference [59]. Figure 4(a) shows the behavior of the eigenvalues near the stability boundary (or flutter boundary) when a moderate (not *very* small) amount of internal, visco-elastic damping is present in the system. (Some external,

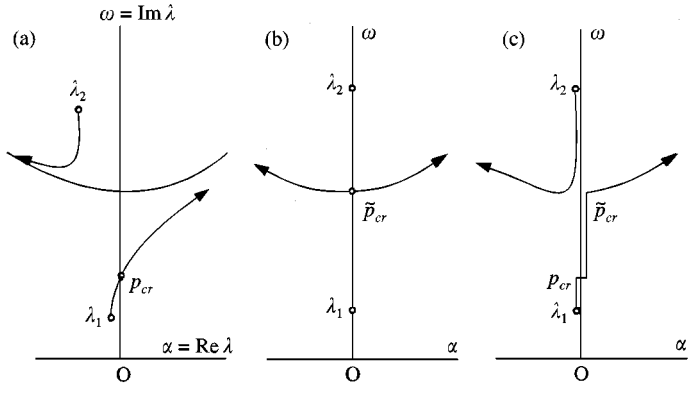

Figure 4. Argand diagrams for Beck's column with different amounts of (internal) damping (from Bolotin and Zhinzher [59]). (a) With a moderate amount of damping; (b) Without damping; (c) With very little damping. In (a), the unstable eigenvalue crosses the imaginary axis at the critical load p_{cr}. The vibrations are asymptotically stable in the load interval $0 < p < p_{cr}$. In (b), flutter is initiated at the "quasi-critical" load $\tilde{p}_{cr}$. The vibrations are just "quasi-stable" in the load interval $0 < p < \tilde{p}_{cr}$. In (c), flutter is initiated at the critical load p_{cr}, but in the load interval $p_{cr} < p < \tilde{p}_{cr}$ the flutter is likely of the "quiet" type, while it is "violent" for $p > \tilde{p}_{cr}$.

viscous damping may also be present.) The load value p_{cr} is termed the critical load in reference [59]. At the load level p_{cr}, one or several *simple* eigenvalues obtain positive real parts ($\alpha > 0$). [The curves have a mirror image in the lower half of the complex plane.]

Figure 4(b) shows the eigenvalue behavior near the flutter boundary for a completely undamped system. Here the two (purely imaginary) eigenvalues coincide on the imaginary axis at the critical load $\tilde{p}_{cr}$. For $p > \tilde{p}_{cr}$, one of the eigenvalues gets a positive real part ($\alpha > 0$), and flutter is initiated. It emphasized that, basically, the vibrations are critical (marginally stable) for all $0 < p < \tilde{p}_{cr}$. (At $p = \tilde{p}_{cr}$ there are solutions proportional to $\exp(i\omega t)$ *and* to $t\exp(i\omega t)$, and the amplitude will thus increase linearly in time at that point.)

Figure 4(c) is for the case with infinitely small internal, visco-elastic damping (infinitely small external, viscous damping may also be present). Here the critical eigenvalue branch is *creeping* along the imaginary axis and is crossing it at the critical value p_{cr}. The "destabilization paradox" is that $(p_{cr})_{\beta,\sigma\to 0}$ (see equation (7) for the definition of β and σ) is much less than $\tilde{p}_{cr}$, about half the value. It is worth noticing that the destabilizing effect of small damping also is known in fluid dynamics. For example, a viscous parallel shear flow may be unstable, while the same inviscid flow is stable [61].

Bolotin and Zhinzher's point of view was that, "it would be more correct to speak not of destabilization, but of false conclusions based on the interpretation of the critical case as the stable one" [59]. They suggested then that, for the undamped case, the load domain should not be considered as "stable", but just as "quasi-stable". Furthermore, $\tilde{p}_{cr}$ should not be called the "critical load", but the "quasi-critical load". Also, they suggested that, in the light of the possible destabilizing effect, it is essential to include damping in all stability investigations, because small internal damping may make the quasi-stable domain unstable. However, if both internal and external damping are very small, the flutter instability in the (before) quasi-stable region may be a "quiet" flutter. In the instability region, the flutter is "violent". Bolotin and Zhinzher emphasized that this hypothesis should be confirmed by the solution of the non-linear problem and by experiment.

The experimental verification has now been given by Sugiyama *et al.* [36]. The key point is that acceptance of "quiet" flutter is equivalent to relaxation of the Lyapunov stability criteria. In reference [36], it was verified by experiment that in

$$p_{cr,damped} < p < p(\alpha_{max}), \quad \alpha_{max} = \ln(n)/t_l > 0 \tag{29}$$

(see equations (27), (28)) the flutter is sufficiently "quiet" to be indistinguishable from the stable state. To exemplify, for one of the experiments in reference [36], criterion (28) gives, with $n = 10$[‡], a non-dimensional critical load of magnitude 12·61. This value is not very different from the theoretical value $p_{cr,undamped} = 12{\cdot}60$ obtained by neglecting damping, but certainly very different from the theoretical value $p_{cr,damped} = 5{\cdot}65$ obtained by including damping. Thus, when the time interval t_l, where the load acts, is small, the destabilizing effect of small damping may not be present in reality. On the other hand, if the load interval t_l is not such a short period, α_{max} must necessarily be very small. As $t_l \to \infty$, p_{cr} smoothly approaches $p_{cr,damped}$. Stability criterion (28) thus eliminates the "destabilizing paradox" present in Lyapunov's stability criteria.

Crandall [62] gave a very interesting account on the importance of damping in engineering systems in general, including non-conservative follower force systems, and destabilizing effects.

[‡] The choice of n, the number of oscillation cycles, is not important.

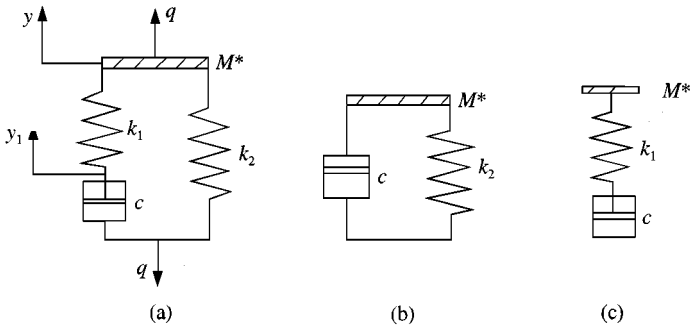

Figure 5. Different viscoelastic foundations to Beck's column, as investigated by Morgan and Sinha [37]. (a) Standard linear solid model, with effective mass M^*, supported by an elastic spring with constant k_1 and a damper with coefficient c, in parallel with another elastic spring with constant k_2; (b) the Kelvin–Voigt model; (c) the Maxwell model.

Morgan and Sinha [37] considered the effect of a viscoelastic foundation on the stability of Beck's column. Three different models were considered; (1) the Maxwell model, which is a spring and a dashpot in series; (2) the Kelvin–Voigt model, which is a spring and a dashpot in parallel; and (3) a "standard linear solid model", which is the Maxwell model coupled in parallel with a spring. The models are shown in Figure 5. Smith and Herrmann [63] found that a continuous, elastic (Winkler) foundation does not increase the critical load of Beck's column; it only increases the flutter frequency. But the combination of continuously distributed springs and dashpots in a Kelvin-Voigt foundation increases the critical load, as seen from Figure 6(a). The Maxwell foundation may also have a stabilizing effect, as illustrated by Figure 6(b). But this effect vanishes as the non-dimensional damping coefficient $C \to \infty$, since the Maxwell foundation then approaches the Winkler foundation. Naturally, the same effect is obtained by the combined "standard linear solid model", as seen from Figures 6(c,d).

External damping has a stabilizing effect in many cases [64]. But Panovko and Sorokin [65] argued that any kind of damping not proportional to $m(x)\,\partial y/\partial t$ (see (equation (1)) may act destabilizing. To exemplify, they considered Beck's column with a single dashpot–damper connected at the free end. It was found that the critical load $p_{cr} \to 10{\cdot}94$ as the damping coefficient $C \to 0$. This interesting example will be discussed further in the following section on energy consideration. A destabilizing effect by "rotary damping" of Beck's column has also been reported [66].

Panovko and Sorokin [65] also considered a relaxed stability criterion similar to that used by Sugiyama *et al.* [36], as discussed in the previous section. So also did Higuchi and Dowell [67] in a study of completely free plates, loaded with a uniformly distributed follower load at one edge. They considered solutions of the form

$$y(x, z, t) = \tilde{y}(x, z)\exp(\mathrm{i}\Omega t), \quad \Omega = \Re(\Omega) + \mathrm{i}\Im(\Omega) = \Omega_R + \mathrm{i}\Omega_I \tag{30}$$

and defined the ratio

$$\Omega_I/\Omega_R \tag{31}$$

as the *true damping rate*. This ratio contains qualitative information about an instability. (Note that it is simply the logarithmic increment (26) of Herrmann and Jong, divided by 2π.) Mathematically, the system is unstable if $\Omega_I/\Omega_R < 0$ (assuming $\Omega_R > 0$). But the smaller the value, the faster will the amplitude of the unstable oscillations grow. In cases where

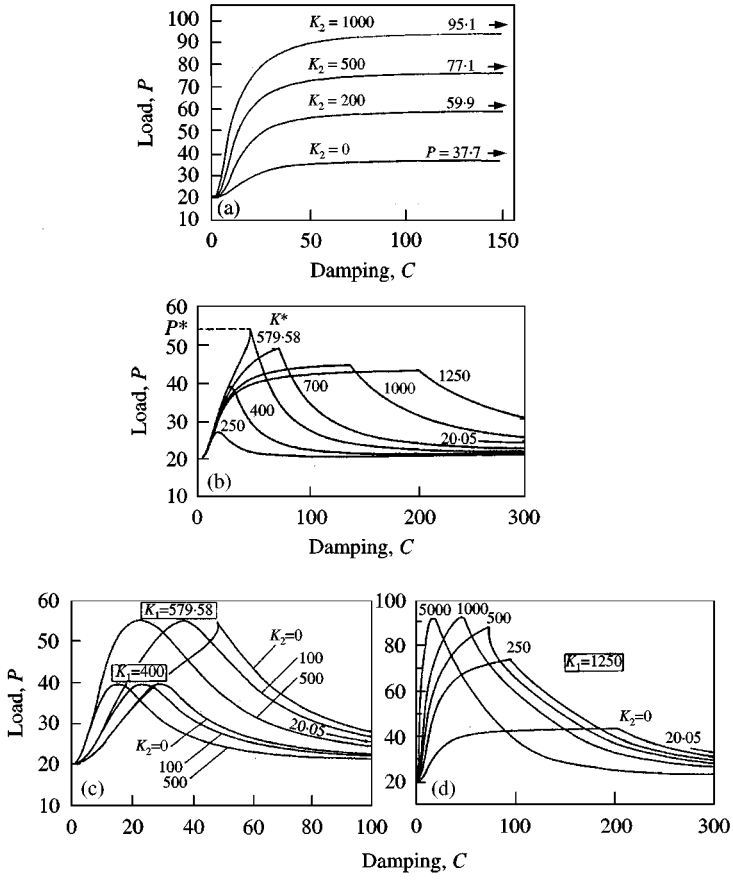

Figure 6. Effects of different viscoelastic foundations on the flutter load of Beck's column (from Morgan and Sinha [37]). The constants K_1, K_2 and C are non-dimensionalized versions of the constants specified in Figure 5. (a) The effect of a Kelvin–Voigt foundation on the flutter load; (b) The effect of a Maxwell foundation on the flutter load. The numbers are values of K_1, $0 \leqslant K_1 \leqslant 1250$; (c, d) The effect of a standard linear solid foundation on the flutter load.

$-\Omega_I/\Omega_R$ is larger than zero, but remains small, Higuchi and Dowell used the name *weak flutter* (which is equivalent to Bolotin and Zhinzher's "quiet flutter" [59]). True stability boundaries $\Omega_I/\Omega_R = 0$ were compared with "relaxed" stability boundaries, defined by $-\Omega_I/\Omega_R = \varepsilon$, where ε is a small, positive number. ($\varepsilon = 0{\cdot}001, 0{\cdot}01$ and $0{\cdot}1$ were used.)

In rounding off this section, we consider again the completely undamped system. As mentioned in connection with Figure 4(b), two imaginary eigenvalues coincide at the flutter load $\tilde{p}_{cr}$. But the corresponding eigenvectors also coincide. Let us denote the two eigensolutions by "1" and "2". Then, at the flutter load,

$$(\lambda_1, y_1) \to (\lambda_f, y_f), \quad (\lambda_2, y_2) \to (\lambda_f, y_f). \tag{32}$$

(Subscript "f" indicates "flutter".) Inserting this in the biorthogonality condition (19) (with damping parameters $\sigma = \beta = 0$) gives the flutter criterion

$$\int_0^1 m y_f v_f \, \mathrm{d}x + \mu[y_f v_f + a(y_f v_f' + y_f' v_f) + (J/\mu + a^2) y_f' v_f']_{x=1} = 0. \tag{33}$$

Equation (18) gives the discretized flutter criterion

$$\mathbf{v}_f^{\mathrm{T}}\mathbf{M}\mathbf{y}_f = 0. \tag{34}$$

2.9. THE INFLUENCE OF GEOMETRY AND VARIOUS BOUNDARY CONDITIONS

Sugiyama *et al.* [68] studied the effect of an elastic support (the clamping at $x = 0$ is changed for a link with a rotational spring), considering both Ziegler's two-degrees-of-freedom model and the continuous Beck's column (without damping). For the continuous model, divergence occurs for $\eta < 0{\cdot}5$ and flutter for $\eta > 0{\cdot}5$, as already mentioned. When the spring stiffness at $x = 0$ is relaxed, the divergence–flutter transition point moves from 0·5 to larger values, and approaches 1·0 when the stiffness approaches 0. Another interesting feature is that for $\eta = 1{\cdot}0$, the critical load has a minimum, $p_{cr} \approx 0{\cdot}8 \times 20{\cdot}05$, at the non-dimensional stiffness value $k_r = KL/EI = 1{\cdot}74$, where K is the spring stiffness.

The same authors also studied the effect of a translational spring fitted at the free end [69]. Also here, both Ziegler's two-degrees-of-freedom model and the continuous model were investigated, but we will again concentrate on the continuous model. When the non-dimensional stiffness value $k_t = KL^3/EI$ (where K is again the spring stiffness) has the moderate value 20, the divergence "nose" moves from $\eta = 0{\cdot}5$ to 0·45, but the flutter boundary line moves under the "nose", such that the shift between divergence and flutter occurs already at $\eta = 0{\cdot}191$. (Compare with Figure 3.) By further increasing the value of k_t, the flutter boundary moves upwards again, and divergence becomes predominant. At $k_t = 35$, the divergence–flutter transition point has moved to 1·03, and at $k_t = 40$, divergence occurs at any value of η. For $\eta = 1{\cdot}0$, the optimum value of k_t is 34·82, and this value corresponds to a flutter–divergence transition point (flutter for smaller values and divergence for larger values, of k_t).

Kounadis [70] and Sato [71, 72] studied the effects of shear deformation and rotatory inertia for Beck's column with elastic spring supports and concentrated masses. These effects have also been studied for Leipholz's column [73].

Ryu and Sugiyama [74] studied the effects of shear deformation and rotatory inertia for Beck's column with an end mass of *finite size*, as described by equation (1). In Ryu *et al.* [75], the same effects were studied for a standing cantilever.

Lee studied the effects of an intermediate spring support [76, 77], tapering and elastic foundation [78], the non-conservativeness parameter η [79], and a relocatable lumped mass [80].

Takahashi [81, 82] studied the dynamic stability of a *cracked* Beck's column. The transfer matrix method was utilized in the analysis. Takahashi and Yoshioka [83] studied the dynamics of *two* coupled Beck's columns, interconnected by two springs. Also in that study, the transfer matrix method was applied.

Sugiyama and Kawagoe [34], and Sugiyama and Mladenov [30] studied the dynamics of columns subjected to the combined action of uniformly distributed vertical and tangential forces, thus generalizing Leipholz's column. Six boundary conditions were considered. At $(x = 0) - (x = L)$ these were: (1) clamped–free,[§] (2) clamped–pinned, (3) clamped–clamped, (4) pinned–pinned, (5) pinned–clamped, and (6) clamped–movably clamped ("roller–skates"

[§] In each case, if supported at $x = L$, this end is movable in the x direction, by means of a 'roller-skate'.

TABLE 1

Divergence–flutter transition points [30]

Case	i	ii	iii	iv	v	vi
Non-conservativeness η	0·5	0·7923	0·8546	1·782	1·974	0·5703

in both the x and the y directions). In all cases, flutter or divergence may occur, depending on the magnitude of the non-conservativeness parameter η. The divergence–flutter transition points are as given in Table 1.

Chen and Ku [84] used the finite element method for an analysis of cantilevered columns with uniformly distributed follower forces.

2.10. FREE–FREE BEAMS WITH A FOLLOWER LOAD

Free–free beams with a follower load at one end mimic the behavior of flexible missiles and space structures propelled by a rocket thrust. The problem was initially studied by Beal [85]. In addition to the beam bending modes, rigid-body translation and rotation is also possible. In papers concentrating on structural dynamic stability, the rigid-body motions are typically assumed to be suppressed by a control system. The issue of a control system was, however, also studied by Beal, by Wu [86, 87] and by Park and Mote [88].

Sugiyama *et al.* [89] studied the effect of internal damping on the flutter boundary for the case of a direction-controlled follower force.

Mladenov and Sugiyama [90] considered a free–free, flexible two-beam system, where the two beams are connected by two springs and two dampers, one of each (coupled in parallel) for the rotational motion, and one of each for the parallel motion. Bending-flutter, post-flutter–divergence and folding instability may occur, depending on the system parameters.

Raju and Rao [91], De Rosa *et al.* [92], and De Rosa [93] considered the dynamics of a simple model of a rocket motor, modelled as a stepped, free–free beam, resting on rotational and translational springs, and having follower forces acting at the step.

2.11. TORSIONAL FLUTTER AND COUPLED TORSIONAL-BENDING FLUTTER

Nemat-Nasser and Herrmann [94] considered a plate-like elastic beam with two follower forces applied symmetrically about the centroid of the cross-section, as sketched in Figure 7. The beam has two axes of symmetry and, accordingly, the equations of motion for lateral and torsional motions are *uncoupled*. The equation for torsional vibrations is

$$EC_w \frac{\partial^4 \phi}{\partial x^4} + (2pr^2 - GJ_t) \frac{\partial^2 \phi}{\partial x^2} + mr^2 \frac{\partial^2 \phi}{\partial t^2} = 0, \tag{35}$$

where EC_w is the warping rigidity, GJ_t is the torsional rigidity, ϕ is the torsional angle, and r is the polar radius of gyration of the cross-section of the beam. The equation for transverse

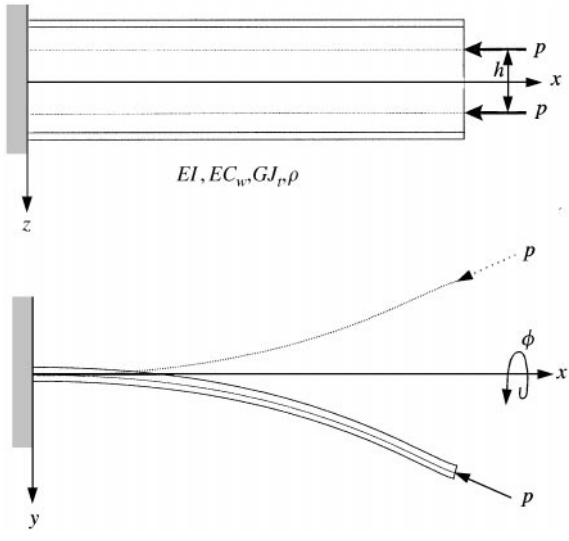

Figure 7. An open cross-section-type cantilevered plate-like beam with two follower forces at the free end (Nemat–Nasser and Herrmann [94]). The beam has length L, bending stiffness EI, torsional stiffness GJ_t, warping stiffness EC_w, and density ρ. The two follower loads, each of magnitude p, are separated by a distance h.

oscillations can be obtained from equation (1). The boundary conditions for the torsional motions are

$$\phi = 0, \quad \frac{\partial \phi}{\partial x} = 0 \quad \text{at } x = 0 \quad \text{and}$$

$$\frac{\partial^2 \phi}{\partial x^2} = 0, \quad EC_w \frac{\partial^3 \phi}{\partial x^3} + \left[p\left(2r^2 - \frac{h^2}{2}\right) - GJ_t \right] \frac{\partial \phi}{\partial x} = 0 \quad \text{at } x = L. \tag{36}$$

Depending on the ratio h/r, where h is the distance between the two follower forces, three types of instability may occur. Torsional buckling occurs for "small" values of h/r, torsional flutter for "moderate" values, and transverse flutter for "large" values.

Beckett and Jayaraman [95] considered a thin, *massless* cantilevered rod subjected to both axial and transverse follower forces and carrying a mass at its free end; see Figure 8. The *coupled* equations of motion for transverse and torsional motions are given by

$$EI \frac{\partial^4 y}{\partial x^4} + p_2 \frac{\partial^2 y}{\partial x^2} - p_1 \frac{\partial^2}{\partial x^2} [(L - x)\phi] = 0 \quad \text{and} \quad GJ_t \frac{\partial^2 \phi}{\partial x^2} + p_1 (L - x) \frac{\partial^2 y}{\partial x^2} = 0 \tag{37}$$

respectively. Here p_1 is the transverse, and p_2 is the axial, follower force respectively. The boundary conditions are

$$y = 0, \quad \frac{\partial y}{\partial x} = 0, \quad \phi = 0 \quad \text{at } x = 0 \quad \text{and}$$

$$\frac{\partial^2 y}{\partial x^2} = 0, \quad EI \frac{\partial^3 y}{\partial x^3} + M \frac{\partial^2 y}{\partial t^2} = 0, \quad GJ_t \frac{\partial \phi}{\partial x} + J \frac{\partial^2 \phi}{\partial t^2} = 0 \quad \text{at } x = L, \tag{38}$$

where J is again the mass moment of inertia of the end-mass M. (Note that there are a couple of misprints in the boundary conditions in the original paper.) The influence of

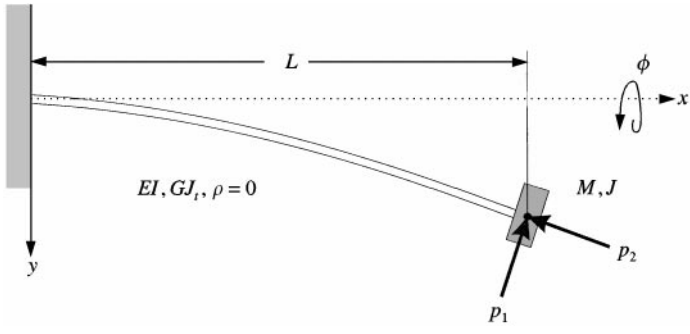

Figure 8. A cantilevered rod with a tangential and a transverse follower force at the free end (Beckett and Jayaraman [95]). The rod, of length L, is weightless, but has bending stiffness EI and torsional stiffness GJ_t. At $x = L$ it has a mass M with rotatory inertial J.

three non-dimensional parameters, $p_* = p_1/p_2$, $p_{**} = p_2L^2/EI$ and L/r (r is the radius of gyration of the end-mass), on the stability/instability boundary is investigated. Coupled torsional-bending flutter occurs for all non-zero values of p_*.

2.12. ENERGETICS

Herrmann and Nemat-Nasser [96, 97] considered the energetics of damped follower-force loaded columns (for Ziegler's pendulum in reference [96], and for Beck's column in reference [97]), much in the spirit of Benjamin's energy-balance analysis of fluid-conveying pipes [98, 99].

An expression for the power delivered by the forces into the structure is obtained by multiplying the force balance (1) by the transverse velocity $\partial y/\partial t$, and integrating over the structure (from $x = 0$ to L). The energy delivered is obtained by integrating the power balance equation over time t. During one period of oscillation, from $t = 0$ to $2\pi/\omega$ say, the energy delivered to the structure is, in physical (dimensional) variables, given by

$$\Delta E = \int_0^{2\pi/\omega} \left[\int_0^L \left\{ E^*I \left(\frac{\partial^3 y}{\partial^2 x\, \partial t} \right)^2 + C \left(\frac{\partial y}{\partial t} \right)^2 \right\} \mathrm{d}x + p \left[\frac{\partial y}{\partial x} \frac{\partial y}{\partial t} \right]_{x=L} \right] \mathrm{d}t. \tag{39}$$

At the critical load, the structure performs periodic, steady state oscillations, with deflections given by

$$y(x, t) = A(x) \cos(\omega t + \theta(x)). \tag{40}$$

Here, ω is the frequency, $A(x)$ is the amplitude and $\theta(x)$ is the phase angle. Thus, at the critical load, $\Delta E = 0$. Equation (39) shows that the damping forces exactly balance the non-conservative force at the critical load, p_{cr}. At $p < p_{cr}$, $\Delta E < 0$, and the vibrations decay. At $p > p_{cr}$, $\Delta E > 0$, and the vibrations grow in amplitude. Roorda and Nemat-Nasser [100] suggested using equation (39) directly for the evaluation of the critical load, and did so for the two-degrees-of-freedom model. (This was also done by Benjamin [98].)

It is very informative to work out equation (39) in greater detail, by inserting solution (40). But it is difficult to extract further information when continuous damping is present. Instead, we will consider the simpler model analyzed by Panovko and Sorokin [65], where

a single dashpot is connected to an otherwise undamped beam at the free end ($x = L$). The damping function $C(x)$ has then the form

$$C\delta(x - L), \tag{41}$$

where δ is Dirac's delta function, and C is a damping parameter independent of x. Inserting expression (41) into equation (39) gives, at $p = p_{cr}$,

$$p_{cr} = -C \frac{\int_0^{2\pi/\omega} (\partial y/\partial t)^2_{x=L} \, dt}{\int_0^{2\pi/\omega} (\partial y/\partial t \, \partial y/\partial x)_{x=L} \, dt}, \tag{42}$$

which, with equation (40) inserted, gives

$$p_{cr} = -C \frac{\omega_{cr}}{(\partial\theta/\partial x)_{x=L}} = C \frac{\omega_{cr}}{k_L} = C c_L. \tag{43}$$

Here k_L and c_L are the wavenumber and the phase velocity, respectively, at $x = L$. Localized damping thus introduces travelling waves in the structure (in contrast to distributed damping). In fact, the dynamics of this system is completely equivalent to that of the cantilevered fluid-conveying pipe [101]. Here the fluid damping is also localized at $x = L$, and the phase velocity at the free end, c_L, equals the critical flow speed U_{cr}. The follower load is proportional to MU^2, where M is the fluid mass per unit pipe length, and U is the fluid speed. The damping is proportional to MU. The critical flow speed U_{cr} corresponds then to the ratio p_{cr}/C.

3. EXPERIMENTS

3.1. REUT'S COLUMN

Experiments with Reut's column were performed first by Feldt *et al.* [102] by using a two-degrees-of-freedom model. The load was realized by the action of an impinging fluid jet. Air was used as the working fluid. An ingenious calibrating system, able to measure the force components in the x and y directions, was constructed. The non-conservativeness of the force depends on the type of impact of the fluid particles onto the rigid end-plate. By elastic impact, the resultant force will be perpendicular to the end-plate at any time. It will then be conservative. This situation can be reached approximately if the end-plate is covered with a very smooth and impenetrable, "reflecting" material, such as glass. By completely inelastic impact, the resultant force will be vertical at any time. It will then be non-conservative. This situation can be reached approximately if the end-plate is covered with a coarse, non-woven, "non-reflecting" material, such as felt carpet.

Sugiyama [103] realized the continuous Reut's column experimentally, also by using an air jet. In the terminology of his paper [103], $\tilde{\eta} = 1$ corresponds to a pure conservative loading and $\tilde{\eta} = 0$ to a pure follower force. Sugiyama obtained the value $\tilde{\eta} = 0{\cdot}7$ by using a glass plate. In a later paper by Sugiyama *et al.* [104], the range of realized $\tilde{\eta}$-values had been increased significantly; $\tilde{\eta} = 0{\cdot}44$ was obtained with abrasive paper, 0·22 with a non-woven material with a fine mesh, and 0·001 with a non-woven material with a coarse mesh. The last case is extremely close to the pure follower load. Flutter occurs for (approximately) $\tilde{\eta} < 0{\cdot}18$ and divergence for $\tilde{\eta} > 0{\cdot}18$. Figure 9 shows a "snapshot" of the flutter motion by $\tilde{\eta} = 0{\cdot}001$, obtained with the aid of electronically controlled flash illumination.

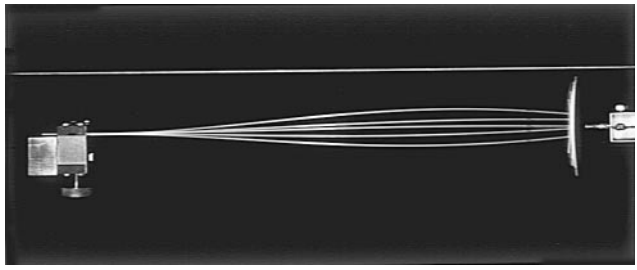

Figure 9. Experimental realization of the continuous Reut's column by means of an impinging air jet (from Sugiyama *et al.* [103–104]). The photograph of the flutter motion was taken with the aid of electronically controlled flash illumination [104].

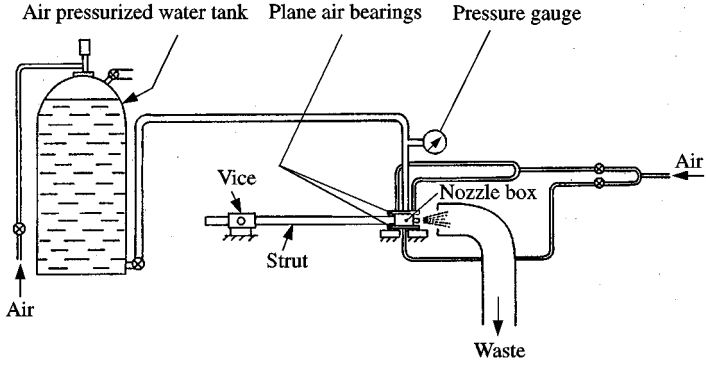

Figure 10. The experimental Beck's column set-up of Wood *et al.* [24].

The effect of localized damping on a two-degree-of-freedom model of Reut's column was studied experimentally by Sugiyama [105]. In that study, $\tilde{\eta} = 0{\cdot}001$ was obtained. A more detailed description is given in reference [106].

As *control systems* become faster and more precise, one might imagine that Beck's column also could be realized by an impinging air jet, where a control system takes care of always keeping the jet tangential to the free end. But time delays cannot be completely eliminated. Kiusalaas and Davis [107] studied the effect of a time delay of the follower force by Zielger's double pendulum. The angle of the force was specified by

$$\frac{\partial}{\partial x} y(L, t - \tau), \tag{44}$$

where τ is a constant time lag. It was shown that this effect is destabilizing, similar to small internal damping.

3.2. BECK'S COLUMN

Bolotin [6] mentioned that, in the early 1960s, several simple demonstration models were made in his laboratory. The source of the jets were cylinders with pressurized air.

An "indirect experimental study" was carried out by Sugiyama *et al.* [108] by means of an analog computer. The mechanical system was thus replaced by an equivalent electronic

circuit. Beck's, Hauger's and Leipholz's columns were investigated and, in general, good agreement between theoretical and simulated values was found.

The first direct, quantitative experimental study of a cantilevered column under a pure follower load seems to be that carried out by Wood *et al.* [24]. The thrust was developed using a water jet, discharged from a so-called nozzle box, attached to the free end. Friction was minimized by using air bearings. The maximum possible thrust was 16 N. The test columns were made of Perspex. Figure 10 shows the set-up. Figure 11 shows a comparison between experimental and theoretical values. The finite size of the nozzle box was taken into consideration in the calculations. In general, the agreement between theory and experiment is good.

Sugiyama *et al.* [36] suggested a more "direct" approach by using a small solid-propellant rocket motor mounted to the free end, as the nozzle box of Wood *et al.* The set-up is shown in Figure 12. Figure 13 shows a sequence of "snapshots" of the flutter motion. The thrust curve for the rocket motor is shown in Figure 14(a). The burn-time is about 4 s. The average thrust is about 40 kgf (392 N), or about 25 times the thrust obtained in reference [24]. The test columns were slender aluminium bars, which have very little damping. Agreement between theory and experiment is very good if the relaxed stability criterion (28) is used. The theoretical stability limit obtained in this way is very close to the result obtained by neglecting damping. That is to say, the destabilizing effect of small damping is not manifested within the very short burning time of the rocket motor.

In the paper by Sugiyama *et al.* [56], the destabilizing effect of an intermediate concentrated mass was verified experimentally. For those experiments, an improved rocket motor, having a much smoother thrust curve (see Figure 14(b)), was developed. The "price" was a shorter burnout time, only 3·2 s. Theoretical and experimental results were in very good agreement.

It is known that the fluid damping associated with a follower-type fluid jet may stabilize vibrations [101, 109]. But a pure follower force may also act stabilizing, rather than destabilizing! Figure 15 shows a standing cantilevered column with an end-mounted rocket motor. Before ignition of the rocket motor, the column is buckled due to its own weight, and

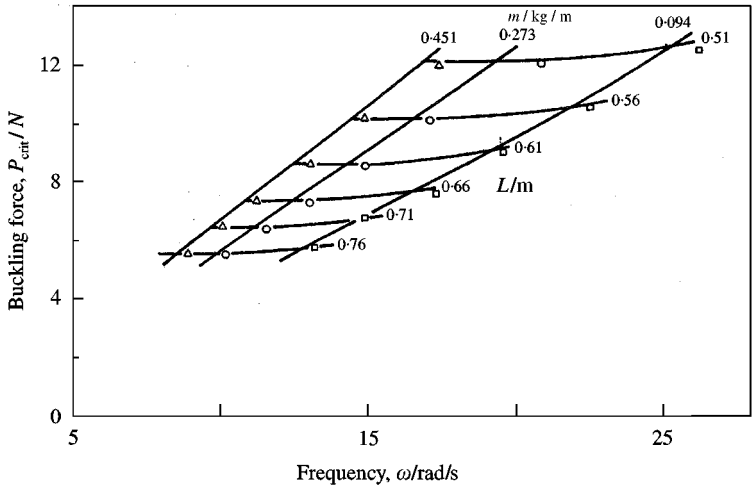

Figure 11. Comparison between theoretical and experimental values for the work of Wood *et al.* [24]. Theoretical values correspond to the intersections of the lines. The experimental values are indicated by △, ○, □.

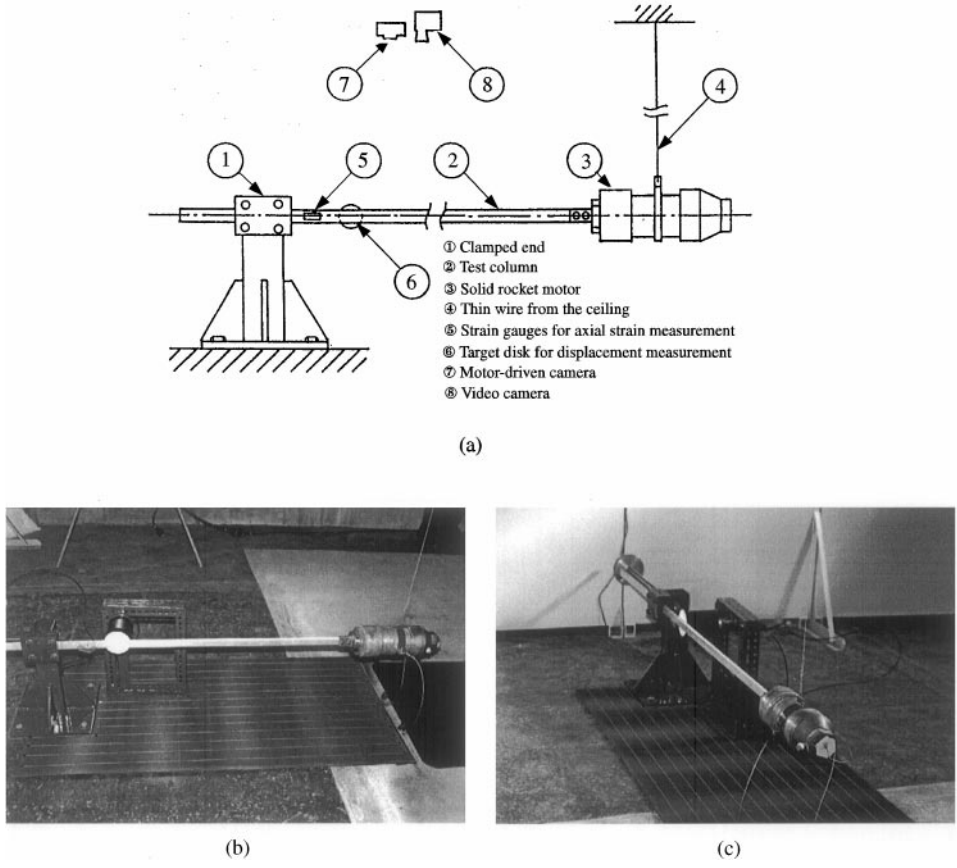

Figure 12. The experimental Beck's column set-up of Sugiyama *et al.* [36]. (a) Schematic; (b) side-view; (c) bird's-eye view.

the weight of the rocket motor. Now consider again the stability map of Figure 3. If a non-conservative load is applied to a buckled beam, it may be possible to move to the right in the diagram, out of the divergence domain and into the stable domain. This idea was verified experimentally by Sugiyama *et al.* [57]. Figure 16 shows the stability map for the experimental system. Before ignition, the rocket motor provides a pure dead load of 14·65 kgf. This is just above the critical load level, and the column is in a buckled state. After ignition, the total compressive load is 54·2 kgf, but the non-conservativeness parameter $\eta = 0{\cdot}74$ and thus, the straight configuration $y(x,t) \equiv 0$ is restabilized due to an increased load level!

A review of the experiments with solid propellant rocket motors, performed at Osaka Prefecture University, was given by Sugiyama [110].

4. OPTIMUM DESIGN

In almost all studies on optimum design of columns subjected to follower loads, no attention has been paid to experimental realization. Still, most of these studies have served an important purpose in the development of optimization techniques for practical,

large-scale optimization problems with non-conservative forces, such as in aeroelasticity [111]. Some experiments have been performed in cases where the follower load was produced by the water jet at the free end of a cantilevered fluid-conveying pipe. Langthjem [112] verified the stabilizing effect of shape optimization of the outer surface of a fluid-conveying pipe. The test-piece was made by turning of a natural-rubber pipe. Borglund [113] verified the shape optimization of slender, beam-like cantilever plates with attached fluid-conveying pipes, and in reference [114], reference is made to some preliminary test-runs with an optimally shaped aluminum cantilever, subjected to the thrust of a small rocket motor.

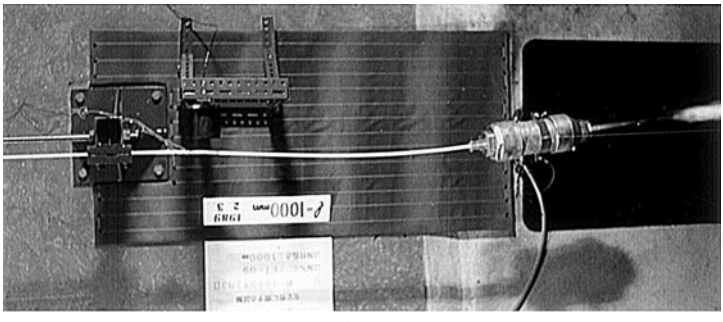

(a)

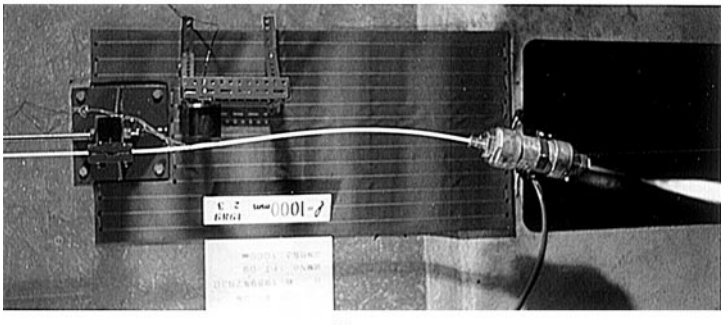

(b)

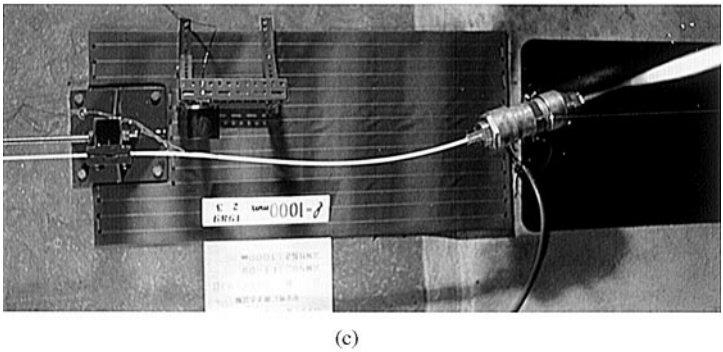

(c)

Figure 13. Fluttering motion observed in the experiments by Sugiyama *et al*. [36]. t is the time that has elapsed after ignition of the solid rocket motor. The corresponding thrust curve is shown in Figure 14(a). (a) $t = 3{\cdot}12$ s; (b) $t = 3{\cdot}36$ s; (c) $t = 3{\cdot}60$ s; (d) $t = 3{\cdot}84$ s; (e) $t = 4{\cdot}08$ s;

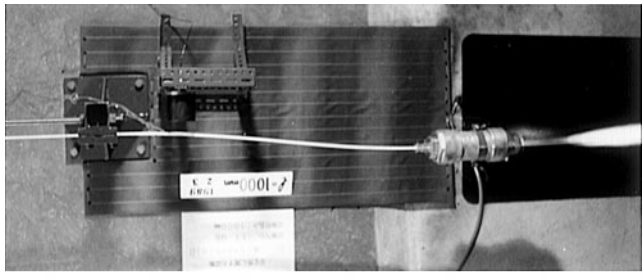

(d)

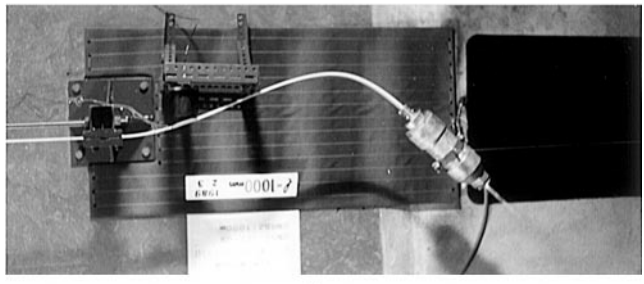

(e)

Figure 13. Continued.

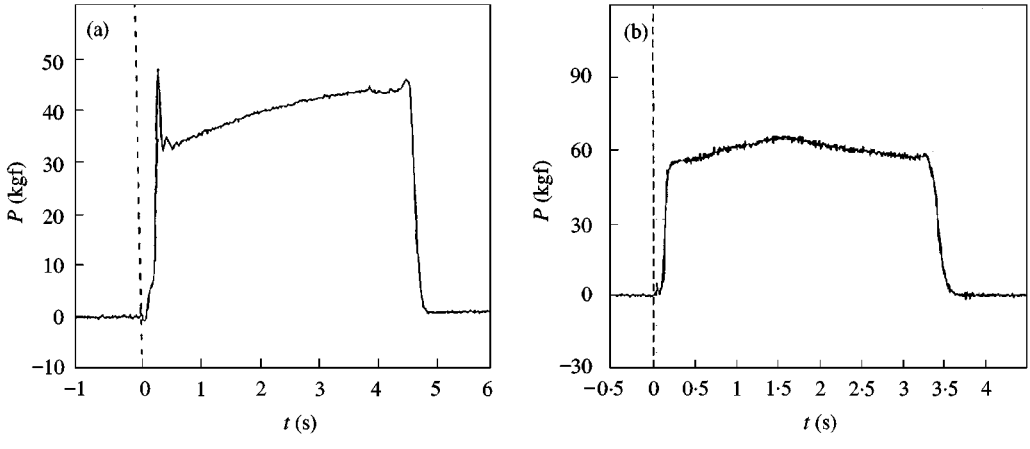

Figure 14. Rocket thrust curves from the experiments by Sugiyama *et al.* (a) from reference [36]; (b) from reference [56].

In general, two different formulations have been considered: (1) maximization of the critical load by constant weight, that is,

$$\max p_{cr}$$

$$\text{subject to weight} = \text{constant},$$

$$p_{cr} \leqslant p_1, p_2, \ldots, p_N; \tag{45}$$

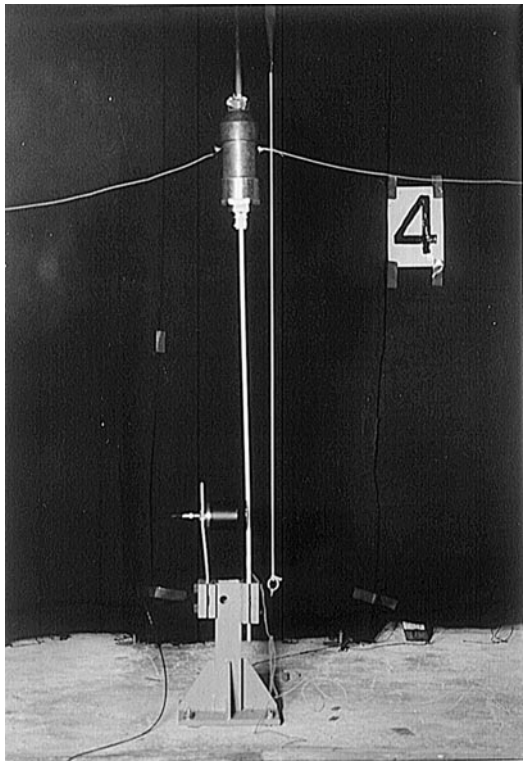

Figure 15. A standing cantilevered column subjected to the weight and the thrust of an end-mounted rocket motor (from Sugiyama *et al.* [57]). The thrust can make a buckled column dynamically stable! The photograph is a "snapshot" of the motion of the test column in its dynamically stable state; the point B shown in Figure 16.

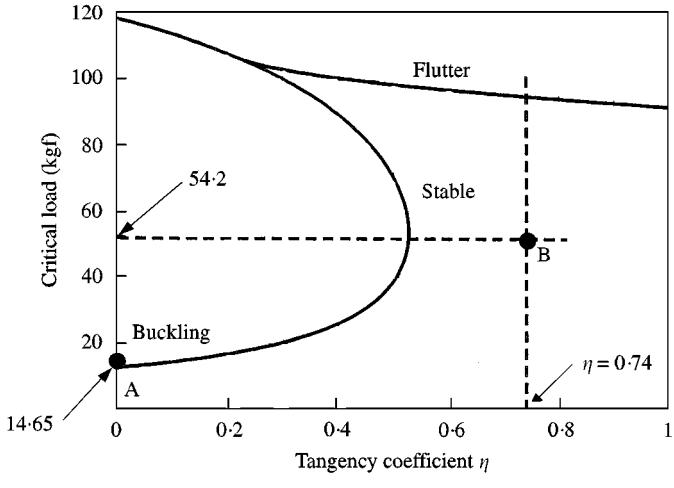

Figure 16. Stability map for the standing cantilever with an end-mounted rocket motor (from Sugiyama *et al.* [57]). The point *A* corresponds to a buckled state under conservative loading. The point *B* corresponds to a dynamically stable state, reached after ignition of the rocket motor.

and (2) minimization of the weight by constant critical load, that is

$$\begin{gathered}\min \text{ weight} \\ \text{subject to } p_{cr} = \text{constant}, \\ p_{cr} \leqslant p_1, p_2, \ldots, p_N. \end{gathered} \tag{46}$$

Here N is the number of unstable eigenvalues. For an *undamped column* these two formulations are completely equivalent. Scaling up the minimum weight design to the initial volume gives the strongest column, and *vice versa*, it being presumed that geometrical constraints different from zero (thickness, say) are not active. This holds true for any type of load. It is most easily proved by considering the equation of motion in discretized form,

$$\mathbf{L}(\mathbf{d})\mathbf{y} = [-\omega^2\mathbf{M}(\mathbf{d}) + \mathbf{K}(\mathbf{d}) + p\mathbf{Q}]\mathbf{y} = \mathbf{0}. \tag{47}$$

(Here $\lambda = 0 + \mathrm{i}\omega$.) We assume that the design variables d_e, collected in the vector $\mathbf{d}$ depend on a common scaling factor ξ, such that

$$\mathbf{d} = \xi\mathbf{d}_0. \tag{48}$$

A general cross-section is considered, with stiffness distribution

$$s(x) = \{m(x)\}^n. \tag{49}$$

For a circular cross-section, $n = 2$, and for a rectangular cross-section with bending about the weakest axis, $n = 1$. For a semi-infinite (infinitely wide) elastic plate, as considered in reference [115], each "strip" behaves as a thin rectangular beam vibrating about the strongest axis, and $n = 3$. The equation of motion (47) can then be written as

$$[-\omega^2\xi\mathbf{M}(\mathbf{d}_0) + \xi^n\mathbf{K}(\mathbf{d}_0) + p\mathbf{Q}]\mathbf{y} = \mathbf{0}. \tag{50}$$

The matrices are thus independent of ξ. The load factor p can be isolated from the equation $\mathbf{v}^{\mathrm{T}}\mathbf{L}\mathbf{y} = 0$, giving

$$p = \xi\,\frac{\mathbf{v}^{\mathrm{T}}(\omega^2\mathbf{M}_0 - \xi^{n-1}\mathbf{K}_0)\mathbf{y}}{\mathbf{v}^{\mathrm{T}}\mathbf{Q}\mathbf{y}}. \tag{51}$$

Here, $\mathbf{M}_0 = \mathbf{M}(\mathbf{d}_0)$ and $\mathbf{K}_0 = \mathbf{K}(\mathbf{v}_0)$. At a flutter load, $\mathbf{b}^{\mathrm{T}}\mathbf{M}\mathbf{u} = 0$ [116], and at a divergence load, $\omega = 0$, so for both kinds of instability onset,

$$p_{cr} = -\,\xi^n\,\frac{\mathbf{v}^{\mathrm{T}}\mathbf{K}_0\mathbf{y}}{\mathbf{v}^{\mathrm{T}}\mathbf{Q}\mathbf{y}}. \tag{52}$$

Thus,

$$\frac{\text{Critical load}}{(\text{Volume of column})^n} = \text{Constant}. \tag{53}$$

4.1. SENSITIVITY ANALYSIS

This is the study of the influence of parameter changes on the characteristics of a physical system. Expressions such as $\partial p_{cr}/\partial m(x)$ and $\partial\omega_{cr}/\partial\beta$ are called sensitivities. The first expression is essential for shape optimization with gradient-based optimization methods. Note that this is the derivative of a scalar with respect to a function, so sensitivity analysis is an extension of the usual concept of derivatives.

Lancaster [43] provided a general "framework" of analysis for general, non-conservative vibratory systems (whose dynamics are described by non-symmetric matrix equations). But that work does not cover multiple eigenvalues, and in undamped follower force problems, flutter occurs through a double eigenvalue. Claudon and Sunakawa [117] considered sensitivity analysis for such double eigenvalue problems. Pedersen and Seyranian [118] gave a unified presentation, covering especially the systems reviewed in this paper. Seyranian [119] developed sensitivity analysis for multiple eigenvalues (not just double). The case where an n-multiple eigenvalue has n linearly independent eigenvectors is called *weak interaction* of these n eigenvalues. On the other hand, if an n-multiple eigenvalue has only one eigenvector, it has $n-1$ so-called associated eigenvectors, which can be determined from the so-called Jordan chain. In that case, the eigenvalues are said to be under *strong interaction*. A strong interaction can be recognized geometrically, because the angle between the eigenvalue branches, in the immediate vicinity of the multiple point, is always π/n. The critical load for an undamped column subjected to a follower force is thus characterized by a strong interaction of two eigenvalues.

Sensitivity analysis has many other potential applications than optimization. Chen and Ku [84, 120–122] suggested a combined Newton–Raphson/bisection iteration method for determining the critical load for an undamped follower force-loaded column. For starting the algorithm, it is assumed that flutter occurs by coincidence of two specific load–frequency curves, for example (p_1, ω_1) and (p_2, ω_2). Let p^* be the initial guess of the critical load. The first approximation to the critical load p_{cr} is taken as

$$p_{cr}^* = p^* + \Delta p, \quad \Delta p = -\frac{\omega_2^2 - \omega_1^2}{\partial(\omega_2^2 - \omega_1^2)/\partial p}. \tag{54}$$

Sensitivity analysis is used to compute $\partial(\omega_2^2 - \omega_1^2)/\partial p$ analytically. The second approximation to p_{cr} is taken as

$$p_{cr}^{**} = (p^* + p_{cr}^*)/2. \tag{55}$$

Steps (54) and (55) are repeated until a specified accuracy criterion is satisfied.

4.2. OPTIMIZATION OF THE CRITICAL LOAD OF THE UNDAMPED BECK'S COLUMN

4.2.1. *Early studies*

The first study of this problem was carried out by Odeh and Tadjbakhsh [123]. Besides considering the optimization problem, they presented some interesting theoretical results, such as a proof of the existence of a critical load for non-uniform columns. Apparently, Odeh and Tadjbakhsh were able to increase the critical load almost 12 times, from 20·05 to 234·48! However, the load–frequency curves (p, ω) were not checked in their study.

Vepa [124] considered the problem in minimum weight formulation, and attempted to derive a general optimality condition for non-conservative systems.

The load maximization problem was studied simultaneously by Sundararajan [125] and by Plaut [126]. Plaut was the first to notice the duality of the problem formulations (45) and (46).

Claudon [127] demonstrated that it is essential to keep track of all load–frequency curves when optimizing. By re-analyzing the optimal column in reference [123], Claudon found that, although the first and second eigenvalue branches coincided at $p = 235{\cdot}48$, the second and third coincided at $p = 6$. It was pointed out that, as the load at which the first and second eigenvalue branches coincide is increased, the load at which the third and the fourth

branches coincide decreases simultaneously. Claudon considered the design where these two load values become equal as being optimal. In this way, $p_{cr} = 57{\cdot}8$ was obtained for the optimal design. (It is the same solution as shown in reference [126].) Later, Hanaoka and Washizu [128] discovered that these two coinciding flutter loads could be increased simultaneously. In this way, they were able to reach $p_{cr} = 83{\cdot}53$. But they also found that, as the optimization is continued to this level, the second and third load–frequency curves (p_2, ω_2) and (p_3, ω_3), respectively, are prone to coincide and cause a significant drop in the critical load level (such as that which happened in the study of Odeh and Tadjbakhsh [123]). Hanaoka and Washizu introduced a discretization by 10 finite elements with piecewise linear cross-section area, which has become a kind of a benchmark model problem for comparing different optimization techniques.

4.2.2. *Further refinements*

Masur and Mroz [129] studied the formulation of optimality conditions. However, the use of such analytical methods has now basically been given up, due to the problem of an unknown number of coinciding flutter points at the critical load for the optimum design.

Bogacz *et al.* [38] considered volume minimization (formulation (46)) for stepped columns. Graphical solutions are given for columns with two segments. (There are then just two design parameters, a length ratio and a diameter ratio.) Some solutions are given for columns with up to four segments, but the solution method is not described. Bogacz *et al.* state that columns with continuous thickness variation are not of much practical utility, contrary to their stepped columns. But from an experimental point of view, the manufacturing of a column with smooth variation in diameter is a small problem in comparison with the realization of the follower force.

Seguchi *et al.* [130] applied the discretized model suggested by Hanaoka and Washizu [128], but used the so-called adjoint variational principle for the shape optimization. In this way the "record" of Hanaoka and Washizu was surpassed slightly, to $p_{cr} = 87{\cdot}34$. Seguchi *et al.* suggested the interesting idea that all frequency couples (ω_1, ω_2), $(\omega_3, \omega_4), \ldots, (\omega_{2n-1}, \omega_{2n})$ must coincide at the critical load for the true (global) optimum design. They also investigated optimum design of Hauger's and Leipholz's columns (see section 4.4).

Tada *et al.* [131] suggested a method to improve the robustness of the optimal Beck's column, that is, to make the optimal column insensitive to small perturbations of the shape. As pointed out by Hanaoka and Washizu [128], the "weak point" is coincidence of the load–frequency curves (p_2, ω_2) and (p_3, ω_3). Tada *et al.* then suggested keeping these branches apart by a specified distance "c", by including the constraint

$$(\log \omega_3^2)_{p=p_i} - (\log \omega_2^2)_{p=p_i} \geqslant c, \quad i = 1, 2, \ldots, n, \tag{56}$$

where $0 < p_1, p_2, \ldots, p_n < p_{cr}$ are some specified load values. With $c = 0{\cdot}5$, the optimum design not only became more robust but also, the "record value" $p_{cr} = 90{\cdot}80$ was obtained.

Gutkowski *et al.* [132] suggested an optimization algorithm which takes advantage of the duality of equations (45) and (46). In every iteration, the volume was minimized under the constraint of constant critical load. Then, before the next iteration, the column was scaled up to the initial volume. In this way, Gutkowski *et al.* reached the critical load $p_{cr} = 92{\cdot}56$. However, the frequency curves ω_2 and ω_3 were very close at $p \approx 70$, making the design very sensitive to small perturbations. Thus, comparing this result to that of Tada *et al.* [131], not so much was gained.

When considering the work described up to this point, it seems that just "higher" and "higher" local optima have been reported. Ringertz [133] carefully checked the solution of

Gutkowski *et al.* [132] and found that their solution was in fact not even a local optimum. Ringertz constructed a design by a linear interpolation of the column of Gutkowski *et al.*, described by the vector $\mathbf{d}_{GMP}$, and a uniform column, described by the vector $\mathbf{d}_0$,

$$\mathbf{d}(\xi) = (1 - \xi)\mathbf{d}_0 + \xi\mathbf{d}_{GMP}. \tag{57}$$

The value $\xi = 0$ gives the uniform column, and $\xi = 1$ gives the column of Gutkowski *et al.* Ringertz found that the strongest column is obtained with the value $\xi = 1{\cdot}261$, which gives the critical load value $p_{cr} = 110{\cdot}8$. Ringertz chose to work with formulation (46) but suggested a new, extended formulation with constraints on the distance between *all* load–frequency curves, at a large number of load values between 0 and p_{cr}. In mathematical terms, the optimization problem was written as

$$\begin{gathered}\min_{\mathbf{d}} V(\mathbf{d}) \geqslant 0, \quad \text{subject to} \\ \text{(a) } \omega_1^2(p_k, \mathbf{d}) \geqslant 0, \quad k = 1, 2, \ldots, n, \\ \text{(b) } \omega_{i+1}^2(p_k, \mathbf{d}) - \omega_i^2(p_k, \mathbf{d}) \geqslant 0, \quad i = 1, 2, \ldots, 2N_e - 1, \\ \text{(c) } \underline{d}_j \leqslant d_j \leqslant \bar{d}_j, \quad j = 1, 2, \ldots, N_e + 1,\end{gathered} \tag{58}$$

where V is the volume of the column, n is again the number of specified control load values, N_e is the number of finite elements, and $\underline{d}_j$ and $\bar{d}_j$ are lower and upper allowable design variables respectively. By using the so-called logarithmic barrier function, problem (58) was transformed into an unconstrained problem, which was solved by using a modified Newton method. An advantage of this approach is that initially distinct eigenvalues cannot merge to cause a discontinuous drop in the critical load. In contrast to all works reported so far, Ringertz did not use a uniform column as initial design, but a slightly modified form of the design of Gutkowski *et al.*, with a critical load of $p_{cr} = 105{\cdot}8$. The optimization algorithm improved this value to $p_{cr} = 188{\cdot}07$. The influence of a refined discretization on the optimum design was also investigated. The results are shown in Table 2.

Ishida and Sugiyama [134] used a 20-element finite element model with linearly varying column diameter (not linearly varying area as in the Hanaoka–Washizu model). They used the problem formulation (45), that is, without constraints on the distance between eigenfrequency branches, but applied a genetic algorithm to solve the optimization problem (in a version called the "constructive algorithm", see also reference [135]). This method has the ability to search for the highest peak in a multipeak function space, and it does not need derivatives of the critical parameters. The resulting optimum design had the critical load value $p_{cr} = 94{\cdot}51$.

Langthjem and Sugiyama [114] studied optimization of a more realistic Beck's column where the follower load is due to an end-mounted rocket motor of finite size. In this case, critical load maximization by constant volume is not identical with volume minimization by

TABLE 2

The critical load as a function of the number of finite elements [133]

N_e	10	20	30	40	50	60	70	80	90	100
p_{cr}	188·07	141·94	143·01	143·52	143·58	143·57	143·57	143·57	143·58	143·59

constant critical load, and the load maximization formulation (45) was considered, including constraints similar to (58b). It was found that by mass-ratios $\mu =$ (mass of rocket motor)/(mass of column) which can be realized experimentally, the critical load can only be increased by a factor of 1·3–1·4. This is similar to what can be obtained in the case of a pure conservative end-load. Also, the great sensitivity to small changes in the design parameters, and the optimization method dependency by Beck's column, are not seen for "practical" values of μ.

4.2.3. *Extended versions of the undamped Beck's column*

Langthjem and Sugiyama [136] computed optimal column shapes for several values of the non-conservativeness parameter η between 0 and 1 (specifically, for $\eta = 0{\cdot}0$, 0·2, 0·4, 0·5, 0·6, 0·8 and 1·0). This problem was originally proposed by Zyczkowski and Gajewski [137], but in that paper they approximated the continuous problem by Ziegler's pendulum [58] and considered only anti-tangential forces ($\eta < 0$) where only divergence instability is possible, not flutter. It was found that by optimization, the instability type changes from divergence to flutter by just a small non-conservative force component ($0 < \eta < 0{\cdot}2$), and the gain of optimization is much larger than by a pure conservative load. For example, by $\eta = 0{\cdot}0$ the critical load can be increased 1·33 times, while by $\eta = 0{\cdot}2$ it can be increased 4·57 times, and by $\eta = 0{\cdot}4$ it can be increased 10·32 times! The main results are summarized in Table 3. The critical load of the uniform reference column is denoted by p_{cr}^0. The instability mechanism is listed in the last column. Here, SMB means "single mode buckling", SFF means "single frequency flutter" and TFF means "two frequencies flutter". SFF means that one pair of load–frequency curves (p, ω) coincide at the critical load; by TFF, two pairs coincide.

4.3. OPTIMIZATION OF THE CRITICAL LOAD OF THE DAMPED BECK'S COLUMN

The first study of this problem was carried out by Plaut [126]. Internal damping was included, with $\sigma = 0{\cdot}01$. External damping was not included. A gradient projection method, similar to the one used for the undamped case, was applied, and the critical load was increased from 10·96 to 27·5.

The same problem was studied by Claudon and Sunakawa [138, 139]. Also here, internal damping was included, with $\sigma = 0{\cdot}01$, and external damping was not included. Claudon and Sunakawa used a Galerkin-type discretization into orthogonal polynomials and a *continuous* design description (implying that numerical integration of the equilibrium

TABLE 3

Summary of the results from reference [136]

η	p_{cr}^0	Min. vol. by p_{cr}^0	Optimal p_{cr} by unit vol.	p_{cr}/p_{cr}^0	Instability
0·00	2·47	0·866	3·29	1·33	SMB
0·20	3·33	0·468	15·21	4·57	SFF
0·40	5·29	0·311	54·58	10·32	SFF
0·50	16·05	0·486	67·96	4·23	TFF
0·60	16·26	0·513	61·78	3·80	TFF
0·80	17·59	0·480	76·35	4·34	TFF
1·00	20·05	0·379	139·30	6·95	TFF

equation was necessary at each design iteration). The optimization method was based on a gradient projection method, taking the two lowest flutter loads, p_1 and p_2, into account. Two examples were considered in reference [138]. For the uniform column, $p_1 = 10{\cdot}96$ and $p_2 = 109{\cdot}9$. In the first example, p_1 was maximized with constant total mass and a fixed value of the second flutter load ($p_2 := 100$) as constraints. By optimization, p_1 was raised to 25·5 (while p_2 drifted slightly, down to 99·5, due to the strongly non-linear character of the problem). In the second example, p_1 and p_2 were optimized simultaneously, and the values $p_1 = p_2 = 39{\cdot}2$ were reached.

Seguchi *et al.* [140] applied the 10-finite-element model of Hanaoka and Washizu, with internal damping $\sigma = 0{\cdot}01$ and external damping $\beta = 1{\cdot}0$. With these values of the damping parameters, the two lowest flutter loads for the uniform column are $p_1 = 17{\cdot}8$ and $p_2 = 112{\cdot}0$ respectively. By using a gradient projection method to obtain the optimum design, these two values changed to $p_1 = 66{\cdot}79$ and $p_2 = 67{\cdot}30$ respectively. However, the critical load is almost a triple flutter load, as $p_3 \approx 68{\cdot}37$.

Langthjem [141] studied the influence of internal and external damping on the optimal design. The equation of motion was discretized by using a generalized Ritz method [40, 41, 118]. The mass distribution was expressed in terms of orthogonal trigonometric functions. That study also revealed that *transference of instability branch* is possible for the damped Beck's column. A detailed mathematical study of this phenomenon, which occurs through collision of eigenvalues, was carried out by Seyranian [142], who cites physical examples from experiments with fluid-conveying pipes by Bishop and Fawzy [9], and Sugiyama and Noda [143].

Ringertz [52] also applied the 10-finite-element model introduced in reference [128] to study minimum weight design of the damped Beck's column. The stability analysis was carried out by making use of the matrix stability criterion (24). As in reference [133], the barrier method was used in the solution of the optimization problem.

Langthjem and Sugiyama [144] considered weight minimization of the damped Beck's column with a constraint on the static buckling load (by a pure conservative loading). The idea was that since the gain by optimization under non-conservative loading is so much larger than that by conservative loading, the optimal column (for non-conservative loading) might become very weak for other types of loads than the design load. In applications, it may be important that the optimal column also is capable of supporting these loads. For example, a space structure may be subjected solely to follower loads in space, but it must be able to carry some dead load while being subjected to the gravity of the Earth. The optimization problem was written as

$$\min_{\mathbf{d}} V(\mathbf{d}) \text{ subject to}$$

$$\text{(i) } p_f \geqslant p_f^0 \quad [\text{by } \eta = 1 \text{ in equation (8)}],$$

$$\text{(ii) } p_b \geqslant c p_b^0 \quad [\text{by } \eta = 0 \text{ in equation (8)}],$$

$$\text{(iii) } \alpha_j \leqslant \begin{cases} -\varepsilon_j & \text{for } \tilde{p} \leqslant p \leqslant p_f - p_* \\ 0 & \text{for } p_f - p_* \leqslant p \leqslant p_f, \quad j = 1, 2, \ldots, 2N_e, \end{cases}$$

$$\text{(iv) } \underline{d}_k \leqslant d_k \leqslant \bar{d}_k, \quad k = 1, 2, \ldots, N_e + 1, \tag{59}$$

where V is again the volume of the column, and p_f^0 and p_b^0 are the flutter load (by pure follower loading) and the buckling load (by pure "dead" loading), respectively, for the

TABLE 4

Summary of results obtained in reference [144]

Slack parameter c	Minimum volume	Flutter load p_f	Buckling load p_b
0·00	0·3585	11·22	0·2200
0·25	0·5146	11·69	0·6169
0·50	0·6415	12·83	1·2337
0·75	0·7534	11·22	1·8506
1·00	0·8664	13·32	2·4674

uniform column. Again, $\alpha_j = \Re(\lambda_j)$ and $\tilde{p}$ and p_* are some chosen load values. Finally, ε_j are small, positive numbers. The buckling constraint (ii) includes a "slack parameter" $c \in [0, 1]$. Setting $c = 0{\cdot}25$, for example, means that the buckling load of the optimal column may not be less than 0·25 times the buckling load of the uniform column. The results are summarized in Table 4. When $c = 1{\cdot}0$, the optimal column is the optimal Euler column, as obtained by Tadjbakhsh and Keller [145].

A continuation of the study by Langthjem and Sugiyama [136], considering the damped Beck's column, is given in reference [146]. With damping, critical load maximization by constant volume and volume minimization by constant critical load are not identical in general, but only in some special cases. Namely, when stability is lost (1) through a simple or a double zero eigenvalue $\lambda = 0$, and (2) through *one* pair of simple, complex conjugate eigenvalues, $\lambda = \pm \mathrm{i}\omega$. As in reference [136], optimization is carried out for $\eta = 0{\cdot}0, 0{\cdot}2, 0{\cdot}4, 0{\cdot}6, 0{\cdot}8$ and $1{\cdot}0$. When optimizing with the η-values 0·2 and 0·4, the divergence–flutter transition point moves from 0·5 to the actual η-value. This is because these points are local optima in the $\eta - p_{cr}$ plane. (Exactly the same situation is seen for the end-mounted spring with optimal stiffness [69], see section 2.9.) For these η-values, as well as for $\eta = 0{\cdot}5$, the optimization is carried out at a non-differentiable double zero eigenvalue. The optimum design changes smoothly with η, although different stability mechanisms are active. The main results are summarized in Table 5. The instability mechanisms are again listed in the last column. SMB means "single mode buckling", D–F means coincidence of divergence and flutter and, as before, SFF means "single frequency flutter", and TFF means "two frequencies flutter". By SFF one eigenvalue branch moves into the unstable region at the critical load (in fact, one pair of complex conjugate eigenvalue branches). By TFF, two branches go into the unstable region simultaneously.

4.4. OPTIMIZATION OF HAUGER'S AND LEIPHOLZ'S COLUMNS

Anderson [147] studied maximization of the critical load of Hauger's column with internal and external damping, assuming a parabolic mass distribution,

$$m(x) = c_1 + c_2(1 - x)^{c_3}, \tag{60}$$

where c_1, c_2 and c_3 are positive constants. The value of c_1 was prescribed and the optimum values of c_2 and c_3 were found for several values of external damping, with fixed value of internal damping. The percentage increase in the critical load was between 53 and 110 for rectangular cross-sections, and between 20 and 54 for circular cross-sections. The optimization problem was solved by using an optimization method devised by Rosenbrock.

TABLE 5

Summary of the results from reference [146]

η	p_{cr}^0	Min. vol. by p_{cr}^0	Optimal p_{cr} by unit vol.	p_{cr}/p_{cr}^0	Instability
0·00	2·47	0·866	3·29	1·33	SMB
0·20	3·33	0·737	6·13	1·84	D–F
0·40	5·29	0·744	9·55	1·81	D–F
0·50	10·07	0·961	10·91	1·08	D–F
0·60	9·59	0·942	10·80	1·13	SFF
0·80	9·77	0·463	45·23	4·63	TFF
1·00	11·22	0·368	68·61	6·11	TFF

Related to this paper are a couple written by Thomas [148, 149], who considered weight minimization of Hauger's column. The damped Hauger's column was reconsidered by Claudon [150], using formulation (45).

Claudon [127] also considered optimum design of the undamped Hauger's column in addition to his important work on the undamped Beck's column. Similar to that study, the load–frequency curves were carefully traced. For the uniform column, the two lowest flutter points are $p_1 = 151$ and $p_2 = 946$ respectively. By optimization the flutter load was raised to $p_{cr} = 425$, but this is a discrete instability where the second and the third eigenvalue branches coincide.

The same problem was reconsidered by Seyranian and Sharanyuk [115] who analyzed the dynamic stability by the finite difference method. By using a gradient projection method, they increased the critical load to 433. Flutter occurs through coincidence of the first and the second eigenvalue branches. By further optimization, the second and the third eigenvalue branches coincide, as also experienced by Claudon [127].

Another analysis of optimum design of Hauger's column was carried out by Seguchi *et al.* [130], using the 10-finite-element model. The critical load was raised to 367. They also considered optimization of Leipholz's column. Here, the critical load was increased from 40·1 to 117.

5. DYNAMIC STABILITY UNDER A PERIODIC FOLLOWER FORCE

The first study of parametric resonance in Beck's column is due to Sugiyama *et al.* [108]. This was an "experimental" study which was conducted by means of an analog computer. The load was prescribed as

$$p(t) = p_1 + p_2 \cos(\Omega t) \tag{61}$$

and the dynamics were investigated for various values of p_1 and p_2. It was found that combination resonances of difference type ($\omega_2 - \omega_1$ and $\omega_3 - \omega_2$, for example) can occur, in addition to simple parametric resonance. Theoretical support of the analog simulations was given later by Sugiyama *et al.* [151]. By applying a discretization method to the equation of motion (the finite difference method was used), a system of N coupled Mathieu equations was obtained,

$$m\frac{\mathrm{d}^2 y_i}{\mathrm{d}t^2} + EI\sum_{j=1}^{N} s_{ij} y_j + (p_1 + p_2\cos(\Omega t))\sum_{j=1}^{N} t_{ij} y_j = 0, \quad i = 1, 2, \ldots, N. \tag{62}$$

Here s_{ij} and t_{ij} are coefficients which depend on the discretization method. The "experimental" predictions of reference [108] were confirmed by making use of Hsu's resonance criteria [152].

The instability boundaries were determined numerically by Iwatsubo *et al.* [153], by making use of direct numerical simulations. The problem was reconsidered by Iwatsubo *et al.* in reference [154]. It was found that combination resonances of difference type can occur between the mth mode and the $(m + 2n - 1)$th mode $(m, n = 1, 2, \dots)$, while sum-type resonances can occur between the mth mode and the $(m + 2n)$th mode. The effect of damping was also considered.

Kim and Choo [155] considered a free–free Timoshenko beam subjected to a pulsating follower force. This is a simple mathematical model of a missile, or a rocket. An intermediate concentrated mass was included, to represent control machinery. The instability regions were determined with the aid of the method of multiple scales. (See, e.g., the book by Nayfeh [156], who also discusses many other methods for the Mathieu equation.) Also here, combination resonances of both sum and difference type were found, in addition to simple parametric resonance. Among many interesting results, it was found that changes in load level, column slenderness and size of the concentrated mass may change a combination resonance from sum type to difference type, or *vice versa*. It is worth noticing that exactly the same problem was studied 10 years earlier by Ryu [32], but unfortunately published only in the Korean language. Ryu's study also includes distributed friction (as mentioned in section 2.2) and direction control of the thrust.

Kang and Tan [33] considered parametric instability of Leipholz's column under four sets of boundary conditions: (1) clamped–free, (2) pinned–pinned, (3) clamped–clamped, and (4) clamped–pinned. The background for this study is disc brake pad instability. The steady state solution was approximated by a Fourier series. By balancing the harmonic terms, an algebraic eigenvalue problem was obtained, and the stability analysis was performed by computing and checking the complex eigenvalues. In addition to simple parametric resonance, cases (1) and (2) exhibit combination resonance of the sum type, while cases (3) and (4) exhibit both sum- and difference-type resonances.

6. NON-LINEAR DYNAMICS

An enormous amount of work has been done on the non-linear dynamics of the follower force-loaded double pendulum. As even the linear dynamics is very interesting and counterintuitive, there are indeed very many interesting non-linear phenomena; see, e.g., references [157, 158]. The non-linear dynamics of Beck's column may be even richer, but studies into this problem are relatively sparse. (However, there are a substantial number of both theoretical and experimental studies of the related fluid-conveying pipe problem [1, 2].)

Rao and Rao [159] determined the exact values of the critical load for Beck's column with a partial follower force, in the non-conservativeness parameter range $0 \leqslant \eta \leqslant 0{\cdot}5$. A closed-form solution was obtained for a geometrically exact non-linear formulation (sometimes called "the elasticum"). In reference [160], the same model was used for a detailed study of the variations in the critical load around the value $\eta = 0{\cdot}5$. Zuo and Hjelmstad [161] showed mathematically, by using the same exact non-linear formulation, that static bifurcations can exist only for $0 \leqslant \eta \leqslant 0{\cdot}5$.

The bifurcation occurring at the flutter limit for Beck's column was analyzed theoretically by Kolkka [162] for the case with external damping only, and by Chen [163] for the case with internal damping. In both cases, the bifurcation is of the supercritical type, meaning that the non-linearities are stabilizing in the vicinity of the flutter boundary.

Andersen and Thomsen [164] studied the effects of a tip mass of finite size on the bifurcation. A fifth order non-linear model was developed and analyzed by the method of multiple scales, and by direct numerical simulation. Furthermore, an independent finite-element model was developed, to check the results. The main results are that increasing rotatory inertia of the tip mass, and increasing the ratio (external damping)/(internal damping), may result in a change of the bifurcation type, from supercritical to subcritical. This means that the non-linearities become destabilizing, and a sufficiently strong disturbance may initiate unstable, flutter-like oscillations at a load level below the critical (as obtained from a linear analysis).

Gasparini *et al.* [165] compared stability maps for the continuous Beck's column with those for two-, three-, four-, five-, and 10-degrees-of-freedom models. The stability analysis for the continuous column was carried out by using both linear and non-linear finite-element models. Vitaliani *et al.* [166] computed very large deformations of beams subjected to transverse follower forces by using the finite-element method.

7. PLATES SUBJECTED TO FOLLOWER FORCES

Higuchi and Dowell [67, 167, 168] studied the dynamic stability of a completely free panel subjected to a follower force distributed along one edge. These studies have application to the dynamics of large space structures, such as solar panels in a solar power station, when they are moved into orbit by rocket thrusters. Kim and Park [169] considered the same problem when the follower loading is acting at an intermediate section of the plate. With the same applications in mind, Bismarck-Nasr [170] investigated cylindrically curved shallow shells subjected to follower forces.

Kim and Kim [171] studied the dynamics of a cantilevered Mindlin plate subjected to a uniformly distributed follower loading at the free edge. Both isotropic and orthotropic plates were considered. In the isotropic case, the loading parameter was non-dimensionalized as $p = p_0 L^2/D$, where p_0 is the physical load, L is the length of the plate, and D is the stiffness. Direct comparison can thus be made with a beam (see equation (7)). A very thin-walled plate is equivalent to a slender beam, with the critical load value 20·05. As the thickness is increased, the critical load approaches asymptotically the level ≈ 52. In the orthotropic case, the loading parameter is non-dimensionalized differently, and it is difficult to compare the results.

The dynamics of disc-brake systems has been studied by Nishiwaki [172], Mottershead and Chan [173], and Lee and Waas [174]. The mathematical model is a rotating annular plate subjected to a stationary frictional follower load. These studies are closely related to those in reference [33], but with emphasis on the dynamics of the disc, rather than the disc-brake pad.

8. FINITE LOAD INCREASE

In all the studies reviewed so far, the load increase is assumed to be quasistatic. Experimental studies indicate a need for investigating the effects of a dynamic increase. Neishtadt and Sidorenko [175] investigated the dynamics of Ziegler's pendulum when the magnitude of the follower force is slowly increasing. Numerical simulations were performed, and it was demonstrated that the stability loss may be delayed, meaning that the dynamically increasing load level may significantly exceed the critical value before unstable

oscillations develop. An input–output function was constructed, which can predict the time delay, given the initial load value.

A continuation of studies along these lines, to deal with continuous systems with follower loads, would be very useful. Investigation of other types of load increments is also desirable.

9. CONCLUSION

This paper has surveyed the dynamics of simple, flexible structural elements subjected to non-conservative forces. Emphasis is on the "canonical problems", Beck's, Reut's, Leipholz's and Hauger's columns, but some studies of plate and shell problems have also been included. The most important applications are: rockets, missiles, slender space structures (solar panels, etc.), and automobile disk and drum brakes. Beck's and Reut's columns have been realized experimentally, and very good agreement between theory and experiments has been found. Leipholz's column is basically realized in an automobile brake system, where noise due to instability is a well-known problem.

Studies of two-degrees-of-freedom models, such as Ziegler's pendulum, have not been categorically included in this paper. Those problems constitute basically an independent area, and to cover it would most likely result in more additional references than the 170-plus references covered here.

Control theory and applications is another area which has not been covered here, although it is related to optimization.

In the future development of the subject, experimental work, and theoretical work closely related to experiments, ought to be intensified. On the experimental side, new ideas for a simple realization of pure follower forces would be extremely important. The experiments which have been reviewed here may inspire and guide a sound refinement of dynamic stability theory.

ACKNOWLEDGMENTS

The authors gratefully acknowledge the following publishers and authors for permission to reproduce figures: Elsevier Science and Professor V. V. Bolotin (Figure 4); Academic Press and Professor S. C. Sinha (Figures 5 and 6); The Royal Society (London) and Mr. P. M. Saunders (Figures 10 and 11). We also would like to thank Professor Niels Olhoff, Aalborg University, for his support of this work. The first author (M.L.) is grateful to Professor Pauli Pedersen, Technical University of Denmark, for having introduced him to the fascinating subject of dynamic stability.

REFERENCES

1. M. P. Païdoussis and G. X. Li 1993 *Journal of Fluids and Structures* **7**, 137–204. Pipes conveying fluid: a model dynamical problem.
2. M. P. Païdoussis 1998 *Fluid–Structure Interactions: Slender Structures and Axial Flow*. London: Academic Press.
3. G. Herrmann 1971 *NASA Contractor Report CR*-1782, *National Aeronautics and Space Administration* (*NASA*). Dynamics and stability of mechanical systems with follower forces.
4. W. T. Koiter 1996 *Journal of Sound and Vibration* **194**, 636–638. Unrealistic follower forces.
5. Y. Sugiyama, M. A. Langthjem and B.-J. Ryu 1999 *Journal of Sound and Vibration* **225**, 779–782. Realistic follower forces.
6. V. V. Bolotin 1999 *Applied Mechanics Review* **52**, R1–R9. Dynamic instabilities in mechanics of structures.

7. Y. SUGIYAMA, K. KASHIMA and H. KAWAGOE 1976 *Journal of Sound and Vibration* **45**, 237–247. On an unduly simplified model in the non-conservative problems of elastic stability.
8. M. BECK 1952 *Zeitschrift für Angewandte Mathematik und Physik* **3**, 225–228 and 476–477. Die Knicklast des einseitig eingespannten, tangential gedrückten Stabes.
9. R. E. D. BISHOP and I. FAWZY 1976 *Philosophical Transactions of The Royal Society* (*London*), *Series A* **284**, 1–47. Free and forced oscillation of a vertical tube containing a flowing fluid.
10. G. HERRMANN 1967 *Applied Mechanics Review* **20**, 103–108. Stability of equilibrium of elastic systems subjected to nonconservative forces.
11. Y. SUGIYAMA and T. SEKIYA 1971 *Journal of the Japan Society for Aeronautical and Space Sciences* **19**, 61–68. Surveys of the experimental studies of instability of elastic systems subjected to nonconservative forces (in Japanese).
12. C. SUNDARARAJAN 1975 *Shock and Vibration Digest* **7**, 89–105. The vibration and stability of elastic systems subjected to follower forces.
13. T. A. WEISSHAAR and R. H. PLAUT 1981 *Optimization of Distributed Parameter Structures* (E. J. Haug and J. Cea, editors), 843–864. Alphen aan den Rijn: Sijthoff and Noordhoff. Structural optimization under nonconservative loading.
14. A. P. SEYRANIAN 1990 *Advances in Mechanics* **13**, 89–124. Destabilization paradox in stability problems of nonconservative systems (in Russian).
15. I. E. GARRICK and W. H. REED III 1981 *Journal of Aircraft* **18**, 897–912. Historical development of aircraft flutter.
16. V. V. BOLOTIN 1963 *Non-conservative Problems of the Theory of Elastic Stability*. Oxford: Pergamon Press.
17. Y. G. PANOVKO and I. I. GUBANOVA 1965 *Stability and Oscillations of Elastic Systems*. New York: Consultants Bureau.
18. H. ZIEGLER 1968 *Principles of Structural Stability*. Waltham, Massachusetts: Blaisdell Publishing Company.
19. K. HUSEYIN 1978 *Vibrations and Stability of Multiple Parameter Systems*. Alphen aan den Rijn: Sijthoff and Noordhoff.
20. H. LEIPHOLZ 1980 *Stability of Elastic Systems*. Alphen aan den Rijn: Sijthoff and Noordhoff.
21. M. S. EL NASCHIE 1990 *Stress, Stability and Chaos in Structural Engineering. An Energy Approach*. New York: McGraw-Hill.
22. Z. P. BAZANT and L. CEDOLIN 1991 *Stability of Structures*. Oxford: Oxford University Press.
23. A. GAJEWSKI and M. ZYCZKOWSKI 1988 *Optimal Structural Design under Stability Constraints*. Dordrecht: Kluwer.
24. W. G. WOOD, S. S. SAW and P. M. SAUNDERS 1969 *Proceedings of the Royal Society* (*London*), *Series A* **313**, 239–248. The kinetic stability of a tangentially loaded strut.
25. K. SEZAWA 1927 *Tokyo Imperial University. Bulletin of Earthquake Research Institute* **3**, 43–53. On the decay of waves in visco-elastic solid bodies.
26. J. A. HUDSON 1980 *The Excitation and Propagation of Elastic Waves*. Cambridge: Cambridge University Press.
27. G. K. BATCHELOR 1967 *An Introduction to Fluid Mechanics*. Cambridge: Cambridge University Press.
28. H. LEIPHOLZ 1962 *Zeitschrift für Angewandte Mathematik und Physik* **13**, 581–589. Die Knicklast des einseitig eingespannten Stabes mit gleichmässig verteilter, tangentialer Längsbelastung.
29. W. HAUGER 1966 *Ingenieur-Archiv* **35**, 221–229. Die Knicklasten elastischer Stäbe unter gleichmäßig verteilten und linear veränderlichen, tangentialen Druckkräften.
30. Y. SUGIYAMA and K. A. MLADENOV 1983 *Journal of Sound and Vibration* **88**, 447–457. Vibration and stability of elastic columns subjected to triangularly distributed sub-tangential forces.
31. M. P. PADOUSSIS 1973 *Journal of Sound and Vibration* **29**, 365–385. Dynamics of cylindrical structures subjected to axial flow.
32. B.-J. RYU 1988 *Ph.D. thesis, Department of Mechanical Engineering, Yonsei University, Seoul, Korea*. Dynamic stability of the free–free Timoshenko beam subjected to a nonconservative force (in Korean).
33. B. KANG and C. A. TAN 2000 *Journal of Sound and Vibration* **229**, 1097–1113. Parametric instability of a Leipholz column under periodic excitation.
34. Y. SUGIYAMA and H. KAWAGOE 1975 *Journal of Sound and Vibration* **38**, 341–355. Vibration and stability of elastic columns under the combined action of uniformly distributed vertical and tangential forces.

35. P. PEDERSEN 1977 *International Journal of Solids and Structures* **13**, 445–455. Influence of boundary conditions on the stability of a column under non-conservative load.
36. Y. SUGIYAMA, K. KATAYAMA and S. KINOI 1995 *Journal of Aerospace Engineering* **8**, 9–15. Flutter of cantilevered column under rocket thrust.
37. M. R. MORGAN and S. C. SINHA 1983 *Journal of Sound and Vibration* **91**, 85–101. Influence of a viscoelastic foundation on the stability of Beck's column: an exact analysis.
38. R. BOGACZ, H. IRRETIER and O. MAHRENHOLTZ 1980 *Ingenieur-Archiv* **49**, 63–71. Optimal design of structures subjected to follower forces.
39. H. MATSUDA, T. SAKIYAMA and C. MORITA 1993 *Zeitschrift für Angewandte Mathematik und Mechanik* **73**, 383–385. Variable cross sectional Beck's column subjected to nonconservative load.
40. S. N. PRASAD and G. HERRMANN 1969 *International Journal of Solids and Structures* **5**, 727–735. The usefulness of adjoint systems in solving nonconservative stability problems of elastic continua.
41. S. N. PRASAD and G. HERRMANN 1972 *International Journal of Solids and Structures* **8**, 29–40. Adjoint variational methods in nonconservative stability problems.
42. G. L. ANDERSON 1973 *Journal of Sound and Vibration* **27**, 279–296. Application of a variational method to dissipative, non-conservative problems of elastic stability.
43. P. LANCASTER 1966 *Lambda-Matrices and Vibrating Systems*. Oxford: Pergamon Press.
44. I. FAWZY and R. E. D. BISHOP 1976 *Proceedings of the Royal Society* (*London*), *Series A* **352**, 25–40. On the dynamics of linear non-conservative systems.
45. C. D. MOTE Jr 1971 *Journal of the Engineering Mechanics Division. Proceedings of ASCE* **97**, 645–656. Nonconservative stability by finite element.
46. R. S. BARSOUM 1971 *International Journal for Numerical Methods in Engineering* **3**, 63–87. Finite element method applied to the problem of stability of a nonconservative system.
47. V. V. BOLOTIN 1995 *Nonlinear Stability of Structures*: *Theory and Computational Techniques*, *CISM Lectures and Courses No.* 342. (A. N. Kounadis and W. B. Krätzig, editors). Wien, New York: Springer-Verlag. Dynamic stability of structures.
48. Y. SAAD 1980 *Linear Algebra and its Applications* **34**, 269–295. Variations on Arnoldi's method for computing eigen elements of large unsymmetric matrices.
49. Y. SAAD 1981 *Mathematics of Computation* **37**, 105–126. Krylov subspace methods for solving large unsymmetric linear systems.
50. Y. SAAD 1984 *Mathematics of Computation* **42**, 567–588. Chesbyshev acceleration techniques for solving nonsymmetric eigenvalue problems.
51. I. GOLDHIRSCH, S. A. ORSZAG and B. K. MAULIK 1987 *Journal of Scientific Computing* **2**, 33–58. An efficient method for computing leading eigenvalues and eigenvectors of large asymmetric matrices.
52. U. T. RINGERTZ 1995 *Proceedings of the First World Congress of Structural and Multidisciplinary Optimization*, (N. Olhoff and G. I. N. Rozvany, editors), 741–748. Oxford: Pergamon Press. Optimization of eigenvalues in nonconservative systems.
53. W. H. PRESS, S. A. TEUKOLSKY, W. T. VETTERLING and B. P. FLANNERY 1992. *Numerical Recipes in Fortran. The Art of Scientific Programming*. Cambridge: Cambridge University Press.
54. G. HERRMANN and I.-C. JONG 1965 *Journal of Applied Mechanics* **32**, 592–597. On the destabilizing effect of damping in nonconservative elastic systems.
55. G. HERRMANN 1971 *Instability of Continuous Systems*, (H. Leipholz, editor), 238–247. Berlin: Springer Verlag. Determinism and uncertainty in stability.
56. Y. SUGIYAMA, J. MATSUIKE, B.-J. RYU, K. KATAYAMA, S. KINOI and N. ENOMOTO 1995 *AIAA Journal* **33**, 499–503. Effect of concentrated mass on stability of cantilevers under rocket thrust.
57. Y. SUGIYAMA, K. KATAYAMA, K. KIRIYAMA and B.-J. RYU 2000 *Journal of Sound and Vibration* Experimental verification of dynamic stability of vertical cantilevered columns subjected to a sub-tangential force (in press).
58. H. ZIEGLER 1952 *Ingenieur Archiv* **20**, 49–56. Die Stabilitätskriterien der Elastomechanik.
59. V. V. BOLOTIN and N. I. ZHINZHER 1969 *International Journal of Solids and Structures* **5**, 965–989. Effects of damping on stability of elastic systems subjected to nonconservative forces.
60. V. V. BOLOTIN 1971 *Instability of Continuous Systems* (H. Leipholz, editor), 349–360. Berlin: Springer-Verlag. Stability of viscoelastic systems subjected to nonconservative forces.
61. P. G. DRAZIN and W. H. REID 1981 *Hydrodynamic Stability*. Cambridge: Cambridge University Press.
62. S. H. CRANDALL 1970 *Journal of Sound and Vibration* **11**, 3–18. The role of damping in vibration theory.

63. T. E. SMITH and G. HERRMANN 1972 *Journal of Applied Mechanics* **39**, 628–629. Stability of a beam on an elastic foundation subjected to a follower force.
64. R. H. PLAUT and E. F. INFANTE 1970 *International Journal of Solids and Structures* **6**, 491–496. The effect of external damping on the stability of Beck's column.
65. Ya. G. PANOVKO and S. V. SOROKIN 1987 *Mechanics of Solids* (*Mekhanika Tverdogo Tela*) **22**, 128–132. Quasi-stability of viscoelastic systems with tracking forces.
66. I. LOTTATI and I. ELISHAKOFF 1987 *Ingenieur-Archiv* **57**, 413–419. On a new 'destabilization' phenomenon: effect of rotary damping.
67. K. HIGUCHI and E. H. DOWELL 1992 *AIAA Journal* **30**, 820–825. Effect of structural damping on flutter of plates with a follower force.
68. Y. SUGIYAMA, S. MAEDA and H. KAWAGOE 1974 *Theoretical and Applied Mechanics* (*Proceedings of the 22nd National Congress for Applied Mechanics*, 1972), 33–45. *Tokyo*: *University of Tokyo Press*. Destabilizing effect of elastic constraint on the stability of nonconservative elastic systems.
69. Y. SUGIYAMA, H. KAWAGOE and S. MAEDA 1975. *Theoretical and Applied Mechanics*, *Vol.* 23 (*Proceedings of the 23rd Japan National Congress for Applied Mechanics*, 1973), (I. Tani and T. Okumura, editors). 125–135. *Tokyo*: *University of Tokyo Press*. Destablizing effect of elastic constraints on the stability of nonconservative elastic systems (II: The effect of elastic support).
70. A. N. KOUNADIS 1977 *Journal of Applied Mechanics* **44**, 731–736. Stability of elastically restrained Timoshenko cantilevers with attached masses subjected to a follower force.
71. K. SATO 1991 *JSME International Journal* **34**, 459–465. Vibration and stability of a clamped-elastically restrained Timoshenko column under nonconservative loading.
72. K. SATO 1996 *Journal of Sound and Vibration* **194**, 623–630. Instability of a clamped-elastically restrained Timoshenko column carrying a tip load, subjected to a follower force.
73. V. SUNDARARAMAIAH and G. VENKATESWARA RAO 1980 *AIAA Journal* **18**, 124–125. Effect of shear deformation and rotatory inertia on the stability of Beck's and Leipholz's columns.
74. B.-J. RYU and Y. SUGIYAMA 1994 *Computers and Structures* **51**, 331–335. Dynamic stability of cantilevered Timoshenko columns subjected to a rocket thrust.
75. B.-J. RYU, K. KATAYAMA and Y. SUGIYAMA 1998 *Computers and Structures* **68**, 499–512. Dynamic stability of Timoshenko columns subjected to subtangential forces.
76. H. P. LEE 1995 *International Journal of Solids and Structures* **32**, 1371–1382. Divergence and flutter of a cantilever rod with an intermediate spring support.
77. H. P. LEE 1996 *Computers and Structures* **60**, 31–39. Effects of damping on the dynamic stability of a rod with an intermediate spring support subjected to follower forces.
78. H. P. LEE 1996 *International Journal of Solids and Structures* **33**, 1409–1424. Dynamic stability of a tapered cantilever beam on an elastic foundation subjected to a follower force.
79. H. P. LEE 1996 *Computer Methods in Applied Mechanics and Engineering* **131**, 147–157. Damping effects on the dynamic stability of a rod subjected to intermediate follower loads.
80. H. P. LEE 1997 *Computer Methods in Applied Mechanics and Engineering* **144**, 23–31. Flutter of a cantilever rod with a relocatable lumped mass.
81. I. TAKAHASHI 1998 *International Journal of Solids and Structures* **35**, 3071–3080. Vibration and stability of a cracked shaft simultaneously subjected to a follower force with an axial force.
82. I. TAKAHASHI 1999 *Computers and Structures* **71**, 585–591. Vibration and stability of non-uniform cracked Timoshenko beam subjected to follower force.
83. I. TAKAHASHI and T. YOSHIOKA 1996 *Computers and Structures* **59**, 1033–1038. Vibration and stability of a non-uniform double-beam subjected to follower forces.
84. L.-W. CHEN and D.-M. KU 1991 *Computers and Structures* **41**, 813–819. Stability analysis of a Timoshenko beam subjected to distributed follower forces using finite elements.
85. T. R. BEAL 1965 *AIAA Journal* **3**, 486–495. Dynamic stability of a flexible missile under constant and pulsating thrusts.
86. J. J. WU 1975 *Journal of Sound and Vibration* **42**, 45–52. On the stability of a free–free beam under axial thrust subjected to directional control.
87. J. J. WU 1976 *Journal of Sound and Vibration* **49**, 141–147. On missile stability.
88. Y.-P. PARK and C. D. MOTE 1985 *Journal of Sound and Vibration* **98**, 247–256. The maximum controlled follower force on a free–free beam carrying a concentrated mass.
89. Y. SUGIYAMA, T. KATAYAMA, H. FUKUDA and R. C. KAR 1989 *Transactions of the Japan Society of Mechanical Engineers* **55**, 243–247. Effect of internal damping on the stability of free–free beams under an end-thrust.

90. K. A. MLADENOV and Y. SUGIYAMA 1997 *Journal of Sound and Vibration* **199**, 1–15. Stability of a jointed free–free beam under end rocket thrust.
91. K. KANAKA RAJU and G. VENKATESWARA RAO 1994 *Journal of Sound and Vibration* **178**, 429–432. Free vibrations of a free–free partially stressed stepped beam with follower forces.
92. M. A. DE ROSA, K. KANAKU RAJU and G. VENKATESWARA RAO 1995 *Journal of Sound and Vibration* **187**, 540–542. Comment on "Free vibrations of a free–free partially stressed stepped beam" (with reply).
93. M. A. DE ROSA 1996 *Journal of Sound and Vibration* **194**, 631–635. Free vibrations of stepped beams with flexible ends, in the presence of follower forces at the step.
94. S. NEMAT-NASSER and G. HERRMANN 1966 *Journal of Applied Mechanics* **33**, 102–104. Torsional instability of cantilevered bars subjected to nonconservative loading.
95. R. BECKETT and G. JAYARAMAN 1970 *Journal of Applied Mechanics* **37**, 189–190. Instability of a cantilevered rod subjected to nonconservative forces.
96. G. HERRMANN and S. NEMAT-NASSER 1967 *Dynamic Stability of Structures* (G. Hermann, editor), 299–308. Oxford: Pergamon Press. Energy considerations in the analysis of stability of nonconservative systems.
97. S. NEMAT-NASSER and G. HERRMANN 1966 *Ingenieur-Archiv* **35**, 17–24. On the stability of equilibrium of continuous systems.
98. T. B. BENJAMIN 1961 *Proceedings of the Royal Society* (*London*), *Series A* **261**, 457–486. Dynamics of a system of articulated pipes conveying fluid. I. Theory.
99. T. B. BENJAMIN 1961 *Proceedings of the Royal Society* (*London*), *Series A* **261**, 487–499. Dynamics of a system of articulated pipes conveying fluid. II. Experiments.
100. J. ROORDA and S. NEMAT-NASSER 1967 *AIAA Journal* **5**, 1262–1268. An energy method for stability analysis of nonlinear, nonconservative systems.
101. M. A. LANGTHJEM and Y. SUGIYAMA 1999 *Journal of Fluids and Structures* **13**, 251–268. Vibration and stability analysis of cantilevered two-pipe systems conveying different fluids.
102. W. T. FELDT, S. NEMAT-NASSER, S. N. PRASAD and G. HERRMANN 1969 *Journal of Applied Mechanics* **36**, 693–701. Instability of a mechanical system induced by an impinging fluid jet.
103. Y. SUGIYAMA 1982 *SM Archives* **7**, 433–465. Buckling of a generalized Reut rod.
104. Y. SUGIYAMA, T. KATAYAMA and B.-J. RYU 1992 *Proceedings of the Dynamics and Design Conference* 1992, 166–170. *Tokyo*: *Japan Society of Mechanical Engineers*: Vibration and stability of columns under nonconservative forces realized by an impinging jet.
105. Y. SUGIYAMA 1987 *Proceedings of the* 24*th Annual Technical Meeting*, *Society of Engineering Science*, (S. L. Koh, editor), 1–7. *Society of Engineering Sciences*, *Inc*. Experiments on the nonconservative problems of elastic stability.
106. Y. SUGIYAMA, S. MATSUMOTO and T. IWATSUBO 1986 *Transactions of the Japan Society of Mechanical Engineers* **52**, 1058–1065. A theoretical and experimental study on the effect of damping in nonconservative stability problems.
107. J. KIUSALAAS and H. E. DAVIS 1970 *International Journal of Solids and Structures* **6**, 399–409. On the stability of elastic systems under retarded follower forces.
108. Y. SUGIYAMA, N. FUJIWARA and T. SEKIYA 1968 *Proceedings of the* 18*th Japan National Congress for Applied Mechanics*, 1968, 113–126. Tokyo: University of Tokyo Press: Studies on nonconservative problems of instability of columns by means of analog computer.
109. Y. SUGIYAMA, T. KATAYAMA, E. KANKI, N. NISHINO and B. ÅKESSON. 1996 *Journal of Fluids and Structures* **10**, 653–661. Stabilization of cantilevered flexible structures by means of an internal flowing fluid.
110. Y. SUGIYAMA 1998 *International Conference on Theoretical*, *Applied*, *Computational and Experimental Mechanics* (*ICTACEM*98), *Kharagpur*, *India*, *Indian Institute of Technology*. Experimental verification of the effect of rocket thrust on the dynamic stability of cantilevered columns.
111. U. T. RINGERTZ 1994 *Structural Optimization* **8**, 16–23. On structural optimization with aeroelasticity constraints.
112. M. A. LANGTHJEM 1996 *Ph.D. thesis*, *Department of Solid Mechanics*, *Technical University of Denmark*. Dynamics, stability and optimal design of structures with fluid interaction.
113. D. BORGLUND 1998 *Journal of Fluids and Structures* **12**, 353–365. On the optimal design of pipes conveying fluid.
114. M. A. LANGTHJEM and Y. SUGIYAMA 1999 *Journal of Sound and Vibration* **226**, 1–23. Optimum shape design against flutter of a cantilevered column with an end-mass of finite size subjected to a non-conservative load.

115. A. P. SEIRANYAN and A. V. SHARANYUK 1983 *Mechanics of Solids.* (*Mechanika Tverdogo Tela*) **18**, 174–182. Sensitivity and optimization of critical parameters in dynamic stability problems.
116. R. H. PLAUT 1972 *AIAA Journal* **10**, 967–968. Determining the nature of instability in nonconservative problems.
117. J.-L. CLAUDON and M. SUNAKAWA 1981 *Optimization of Distributed Parameter Structures*, (E. J. Haug and J. Cea, editors), 1516–1538. Alphen aan den Rijn: Sijthoff and Noordhoff. Design sensitivity analysis for distributed parameter structural systems governed by double eigenvalue problems.
118. P. PEDERSEN and A. P. SEYRANIAN 1983 *International Journal of Solids and Structures* **19**, 315–335. Sensitivity analysis for problems of dynamic stability.
119. A. P. SEYRANIAN 1993 *Mechanics of Structures and Machines* **21**, 261–284. Sensitivity analysis of multiple eigenvalues.
120. L.-W. CHEN and D.-M. KU 1992 *Journal of Sound and Vibration* **153**, 403–411. Eigenvalue sensitivity in the stability analysis of Beck's column with a concentrated mass at the free end.
121. M. S. JANKOVIC, L.-W. CHEN and D.-M. KU 1993 *Journal of Sound and Vibration* **167**, 557–559. Comments on "Eigenvalue sensitivity in the stability analysis of Beck's column with a concentrated mass at the free end" (and reply).
122. L.-W. CHEN and D.-M. KU 1994 *ASME Journal of Vibrations and Acoustics* **116**, 168–172. Stability of nonconservative elastic systems using eigenvalue sensitivity.
123. F. ODEH and I. TADJBAKHSH 1975 *Journal of Optimization Theory and Application* **15**, 103–118. The shape of the strongest column with a follower load.
124. K. VEPA 1973 *Journal of Structural Mechanics* **2**, 229–257. Generalization of an energetic optimality condition for non-conservative systems.
125. C. SUNDARARAJAN 1975 *Journal of Optimization Theory and Applications* **16**, 355–378. Optimization of a nonconservative elastic system with stability constraints.
126. R. H. PLAUT 1975 *Optimization in Structural Design* (A. Sawczuk and Z. Mroz, editors), 168–180. Berlin: Springer-Verlag. Optimal design for stability under dissipative, gyroscopic, or circulatory loads.
127. J.-L. CLAUDON 1975 *Journal de Mécanique* **14**, 531–543. Characteristic curves and optimum design of two structures subjected to circulatory loads.
128. H. HANAOKA and K. WASHIZU 1980 *Computers and Structures* **11**, 473–480. Optimum design of Beck's column.
129. E. F. MASUR and Z. MROZ 1979 *International Journal of Solids and Structures* **15**, 503–512. Non-stationary optimality conditions in structural design.
130. Y. SEGUCHI, Y. TADA, and K. KEMA 1984 *Transactions of the Japan Society of Mechanical Engineers, Series A* **50**, 679–686. Shape decision of nonconservative structural systems by the inverse variable principle.
131. Y. TADA, R. MATSUMOTO and A. OKU 1988 *Computer Aided Optimum Design of Structures: Recent Advances*, 13–21. *Southampton: Comp. Mech. Publications.* Shape determination of nonconservative structural systems (determination of optimum shape with stable critical load).
132. W. GUTKOWSKI, O. MAHRENHOLTZ and M. PYRZ 1993 *Optimization of Large Structural Systems*, (G. I. N. Rozvany, editor), 1087–1100. Dordrecht: Kluwer. Minimum weight design of structures under nonconservative forces.
133. U. T. RINGERTZ 1994 *Structural Optimization* **8**, 120–124. On the design of Beck's column.
134. R. ISHIDA and Y. SUGIYAMA 1997 *Transactions of the Japan Society of Mechanical Engineers* **63**, 195–200. On the optimal shape of a column subjected to a follower force.
135. R. ISHIDA and Y. SUGIYAMA 1995 *AIAA Journal* **33**, 401–406. Proposal of constructive algorithm and discrete shape design of the strongest column.
136. M. A. LANGTHJEM and Y. SUGIYAMA 2000 *Computers and Structures* **74**, 385–398. Optimum design of cantilevered columns under the combined action of conservative and nonconservative loads. Part I. The undamped case.
137. M. ZYCZKOWSKI and A. GAJEWSKI 1971 *Instability of Continuous Systems* (H. Leipholz, editor), 295–301. Berlin: Springer-Verlag. Optimal structural design in non-conservative problems of elastic stability.
138. J.-L. CLAUDON and M. SUNAKAWA 1981 *Theoretical and Applied Mechanics, Vol.* 30 (*Proceedings of the* 30th *Japan National Congress for Applied Mechanics*, 1980), 263–272. *Tokyo: University of Tokyo Press.* A distributed gradient projection method for optimal design of nonconservative structures.

139. J.-L. CLAUDON and M. SUNAKAWA 1981 *AIAA Journal* **19**, 957–959. Optimizing distributed structures for maximum flutter load.
140. Y. SEGUCHI, M. TANAKA, S. KOJIMA and H. TAKAHASHI 1989 *Transactions of the Japan Society of Mechanical Engineers Series A* **55**, 656–663. Shape determination of a cantilever column subjected to follower force.
141. M. LANGTHJEM 1994 *Structural Optimization* **7**, 227–236. On the influence of damping in an problem of dynamic stability optimization.
142. A. P. SEIRANYAN 1994 *Journal of Applied Mathematics and Mechanics* **58**, 805–813. Collisions of eigenvalues in linear oscillatory systems.
143. Y. SUGIYAMA and T. NODA 1981 *Bulletin of the Japan Society of Mechanical Engineers* **24**, 1354–1362. Studies on stability of two-degrees-of-freedom articulated pipes conveying fluid.
144. M. A. LANGTHJEM and Y. SUGIYAMA 1999 *Structural Optimization* **18**, 228–235. Optimal design of Beck's column with a constraint on the static buckling load.
145. I. TADJBAKHSH and J. B. KELLER 1962 *Journal of Applied Mechanics* **29**, 159–164. Strongest columns and isoparametric inequalities for eigenvalues.
146. M. A. LANGTHJEM and Y. SUGIYAMA 2000 *Computers and Structures* **74**, 339–408. Optimum design of cantilevered columns under the combined action of conservative and nonconservative loads. Part II: The damped case.
147. G. L. ANDERSON 1974 *Journal of Sound and Vibration* **33**, 155–169. Optimal design of a cantilever subjected to dissipative and non-conservative forces.
148. C. R. THOMAS 1975 *Journal of Sound and Vibration* **43**, 483–498. Mass optimization of non-conservative cantilever beams with internal and external damping.
149. C. R. THOMAS 1976 *Journal of Sound and Vibration* **47**, 395–401. Stability and mass optimization of non-conservative Euler beams with damping.
150. J.-L CLAUDON 1978 *Zeitschrift für Angewandte Mathematik und Physik* **29**, 226–236. Determination and maximization of the critical load of a Hauger column in the presence of damping.
151. Y. SUGIYAMA, T. IWATSUBO and K. ISHIHARA 1982 *Journal of Sound and Vibration* **84**, 301–303. Parametric resonances of a cantilevered column under a periodic tangential force.
152. C. S. HSU 1963 *Journal of Applied Mechanics* **30**, 367–372. On the parametric excitation of a dynamic system having multiple degrees of freedom.
153. T. IWATSUBO, Y. SUGIYAMA and K. ISHIHARA 1972 *Journal of Sound and Vibration* **23**, 245–257. Stability and non-stationary vibrations of columns under periodic loads.
154. T. IWATSUBO, Y. SUGIYAMA and S. OGINO 1974 *Journal of Sound and Vibration* **33**, 211–221. Simple and combination resonances of columns under periodic axial loads.
155. J.-H. KIM and Y.-S. CHOO 1998 *Journal of Sound and Vibration* **216**, 623–636. Dynamic stability of a free–free Timoshenko beam subjected to a pulsating follower force.
156. A. H. NAYFEH 1993 *Introduction to Perturbation Techniques*. New York: John Wiley & Sons. Inc.
157. J. J. THOMSEN 1994 *Journal of Sound and Vibration* **188**, 385–405. Chaotic dynamics of the partially follower-loaded elastic double pendulum.
158. J. J. THOMSEN 1997 *Vibrations and Stability, Order and Chaos*. London: McGraw-Hill.
159. B. NAGESWARA RAO and G. VENKATESWARA RAO 1987 *Journal of Sound and Vibration* **120**, 197–200. Applicability of the static or dynamic criterion for the stability of a cantilever column under a tip-concentrated subtangential follower force.
160. B. NAGESWARA RAO and G. VENKATESWARA RAO 1988 *Journal of Sound and Vibration* **125**, 181–184. Stability of a cantilever column under a tip-concentrated subtangential follower force, with the value of subtangential parameter close to or equal to 1/2.
161. Q. H. ZUO and K. D. HJELMSTAD 1997 *Journal of Sound and Vibration* **203**, 899–902. Conditions for bifurcation of a cantilever beam subjected to generalized follower loads: geometrically exact approach.
162. R. W. KOLKKA 1984 *International Journal of Non-Linear Mechanics* **19**, 497–505. On the non-linear Beck's problem with external damping.
163. M. CHEN 1987 *Nonlinear Analysis Theory, Methods and Applications* **11**, 1061–1073. Hopf bifurcation in Beck's problem.
164. S. B. ANDERSEN and J. J. THOMSEN 2000 *Danish Center for Applied Mathematics and Mechanics*, Report No. 635. Post-critical behavior of Beck's column with a tip mass.
165. A. M. GASPARINI, A. V. SAETTA and R. V. VITALIANI 1995 *Computer Methods in Applied Mechanics and Engineering* **124**, 63–78. On the stability and instability regions of non-conservative continuous system under partially follower forces.

166. R. V. VITALIANI, A. M. GASPARINI and A. V. SAETTA 1997 *International Journal of Solids and Structures* **34**, 2497–2516. Finite element solution of the stability problem for nonlinear undamped and damped systems under nonconservative loading.
167. K. HIGUCHI and E. H. DOWELL 1989 *Journal of Sound and Vibration*, **129**, 255–269. Effects of the Poisson ratio and negative thrust on the dynamic stability of a free plate subjected to a follower force.
168. K. HIGUCHI and E. H. DOWELL 1990 *AIAA Journal* **28**, 1300–1305. Dynamic stability of a rectangular plate with four free edges subjected to a follower force.
169. J.-H. KIM and J.-H. PARK 1998 *Journal of Sound and Vibration* **209**, 882–888. On the dynamic stability of rectangular plates subjected to intermediate follower forces.
170. M. N. BISMARCK-NASR 1995 *AIAA Journal* **33**, 355–360. Dynamic stability of shallow shells subjected to follower forces.
171. J. H. KIM and H. S. KIM 2000 *Computers and Structures* **74**, 351–363. A study on the dynamic stability of plates under a follower force.
172. M. NISHIWAKI 1993 *Proceedings of the Institution of Mechanical Engineers* **207**, 195–202. Generalized theory of brake noise.
173. J. E. MOTTERSHEAD and S. N. CHAN 1995 *ASME Journal of Vibration and Acoustics* **117**, 161–163. Flutter instability of circular discs with frictional follower loads.
174. D. LEE and A. M. WAAS 1997 *International Journal of Mechanical Sciences* **39**, 1117–1138. Stability analysis of a rotating multi-layer annular plate with a stationary frictional follower load.
175. A. I. NEISHTADT and V. V. SIDORENKO 1997 *Journal of Applied Mathematics and Mechanics* **61**, 15–25. Stability loss delay in a Ziegler system.